Review | Open Access

Greenverse Science

Qu *et al. Greenverse Sci.* **2026**, *1*, 16 **DOI:**10.20517/greenvsci.2026.11

Structural modulation of metal-organic framework glasses for alkali metal ion transport and conduction

Hanyu Qu[1], Wengang Huang[1,2,*], Jingwei Hou[1,2,*]

Keywords:
Metal-organic framework, MOF glass, ion conduction

Citation: Qu, H.; Huang, W.; Hou, J. Structural modulation of metal-organic framework glasses for alkali metal ion transport and conduction. *Greenverse Sci.* **2026**, *1*, 16. https://dx.doi.org/10.20517/greenvsci.2026.11

Received: 20 May 2026
First Decision: 23 Jun 2026
Revised: 13 Aug 2026
Accepted: 21 Aug 2026
Published: 16 Sep 2026

Academic Editor:
Dengsong Zhang
Copy Editor:
Tong Wang
Production Editor:
Tong Wang

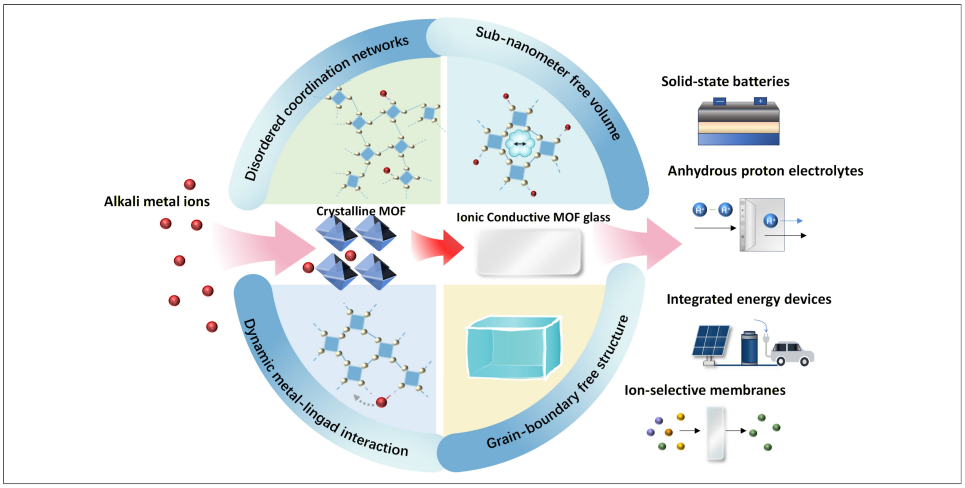

Abstract

Metal-organic framework (MOF) glasses have distinguished themselves as an emerging class of amorphous coordination materials that combine the chemical tunability of MOFs with the processability of glassy solids. Unlike crystalline MOFs, where ion migration is dominated by periodic pore architectures, ion conduction in MOF glasses is expected to arise from the interplay among disordered coordination networks, sub-nanometer free volume, dynamic metal-ligand interactions, and macroscopically grain-boundary-free monolithic structures. This review discusses the structural regulation of MOF glasses for alkali-metal-ion transport, with emphasis on coordination-environment modulation, free-volume control, glass-transition dynamics, and interface-mediated transport. We further highlight the importance of electrochemical and structural characterization, including humidity-dependent impedance spectroscopy, isotope effects, pair distribution function (PDF), extended X-ray absorption fine structure (EXAFS), and positron annihilation lifetime spectroscopy (PALS), to establish reliable structure-transport relationships. We outline future opportunities for MOF-glass ion conductors in anhydrous proton electrolytes, solid-state batteries, ion-selective membranes, and integrated energy devices, calling for a transition from empirical materials discovery to predictable and device-oriented ion-channel design.

[1]Nanomaterials Centre, School of Chemical Engineering, the University of Queensland, Brisbane 4072, Australia.
[2]ARC Centre of Excellence for Green Electrochemical Transformation of Carbon Dioxide, Brisbane 4072, Australia.

[*]**Correspondence to:** Dr. Wengang Huang, Assoc. Prof. Jingwei Hou, Nanomaterials Centre, School of Chemical Engineering, the University of Queensland, Brisbane 4072, Australia. E-mail: wengang.huang@uq.edu.au; jingwei.hou@uq.edu.au

INTRODUCTION

Batteries underpin modern energy storage technologies; however, the realization of solid-state electrolytes (SSEs) that concurrently deliver high ionic conductivity, safety, and processability remains a major challenge[1-3]. Currently, SSEs can be broadly categorized into three types: oxides (ionic conductivity ~10^{-4}-10^{-3} S·cm^{-1}), sulfides (ionic conductivity ~10^{-3}-10^{-2} S·cm^{-1}), and polymers (ionic conductivity ~10^{-7}-10^{-5} S·cm^{-1}). Oxide electrolytes exhibit excellent chemical stability and mechanical strength, but suffer from brittleness, high interfacial resistance, and processing difficulties[4]. Sulfide electrolytes provide high ionic conductivity and good interfacial contact due to their softness, yet they often lack air stability and chemical robustness[5]. Polymer electrolytes are flexible and easy to process; however, they generally exhibit low ionic conductivity at room temperature and limited thermal stability. As a result, none of these systems can simultaneously achieve high conductivity, stability, and processability.

In this context, there is a growing need to explore alternative solid electrolytes. Against this backdrop, metal-organic frameworks (MOFs) have emerged as a versatile platform for developing next-generation solid electrolytes. MOFs are a class of porous materials constructed from metal nodes interconnected by multidentate organic linkers through coordination bonds[6]. Evidence supporting ionic conduction in crystalline MOFs mainly originates from their interconnected pore channels, tunable coordination environments, and chemically functionalized internal surfaces[7-9]. Long-range ordered nanochannels can serve as continuous transport pathways for charge carriers such as Li^+, Na^+, and H^+. Open metal sites within the framework are able to interact with guest salts or ionic liquids, promoting ion dissociation and reducing migration barriers[10,11].

Despite these advantages, crystalline MOFs still face several intrinsic limitations as ionic conductors. Their highly ordered coordination structures are generally rigid and exhibit limited structural flexibility, restricting dynamic ion migration and cooperative rearrangement during transport[12-14]. In addition, ideal crystalline frameworks usually possess relatively low defect concentrations and limited free volume, whereas efficient ionic transport often benefits from higher dynamically disordered environments[15-18]. In practical applications, abundant grain boundaries can interrupt continuous conduction pathways and generate significant interfacial resistance[19-21]. Hence, the ionic transport within many crystalline MOFs is strongly anisotropic resulting in reduced macroscopic transport efficiency.

Compared with crystalline MOFs, MOF glasses possess isotropic, macroscopically grain-boundary-free networks and higher levels of structural disorder, which may provide more continuous pathways for ion transport[22,23]. Earlier works found that there are a high density of defective Zn sites with coordination numbers lower than 4 on the surface of ZIF-62 glass, and they are more uniformly distributed on the glass surface compared to crystalline ZIF-62 surfaces, thereby forming more uniform ionic interactions than crystalline grain-boundary-dominated ZIF-62[24-26]. The developed pore networks of MOF glass also have great accommodation ability for guest species, which attracts much attention towards their use as cations conductors[27]. Consequently, MOF-glass-based materials can exhibit Li^+ ionic conductivities (~10^{-5}-10^{-3} S·cm^{-1}) that exceed those of conventional Li^+-conducting polymer electrolytes (~10^{-6}-10^{-4} S·cm^{-1}) under comparable conditions[28-30]. On the other hand, their macroscopically grain-boundary-free amorphous networks can provide more isotropic ion-transport pathways and reduce interfacial heterogeneity, which is beneficial for long-term cycling stability. Meanwhile, retained short-range metal-ligand coordination motifs offer defined ion-coordination environments, while the disordered glassy matrix improves mechanical integrity and processability. The modular chemistry of MOFs also allows metal nodes, organic linkers, and incorporated salts or ionic liquids to be tailored to enhance electrochemical stability and electrode compatibility. Together, these features make MOF glasses promising SSE platforms with potential advantages in long-term viability, electrochemical stability, and chemical durability.

Ion transport properties in MOF glass are highly related to the pores, ligands and metal sites. This review will provide a critical view of the recent developments in MOF glass for ion transport applications, which is an important area driving the sustainable energy future. We will shed light on the important factors that need to be considered for these materials to obtain enhanced ion transport

properties. Furthermore, we will provide prospective tuning strategies and future research opportunities for developing MOF glass in this area.

Although this review primarily focuses on alkali metal ion transport in MOF glasses, selected examples of proton-conducting MOFs and MOF-derived glasses are also discussed where relevant. Proton transport is included not as a parallel focus, but as a mechanistic reference because it represents one of the most extensively studied forms of ion conduction in MOF-based materials. In particular, proton-conducting systems provide useful insights into how framework flexibility, hydrogen-bond networks, guest molecules, defects, and confined free volume can regulate ion migration in porous or glassy coordination networks. These concepts are relevant to alkali metal ion conduction, even though the charge carriers, transport mechanisms, and coordination environments differ substantially. Therefore, proton-conduction studies are considered here only to extract transferable structure-transport principles that may inform the design of alkali-metal-ion-conducting MOF glasses.

STRUCTURE FEATURES OF MOF GLASSES RELEVANT TO ION CONDUCTION

Disordered coordination networks in MOF glasses

Disordered coordination networks are regarded as one of the defining structural characteristics of MOF glasses and are fundamentally distinct from the highly periodic frameworks observed in crystalline MOFs. Unlike crystalline counterparts that rely on long-range periodic ordering, MOF glasses generally preserve only short-range ordering around the metal coordination environment while exhibiting substantial long-range disorder throughout the extended framework. For example, in ZIF-derived glasses, Zn-N coordination and tetrahedral Zn-imidazolate local structures are often preserved after glass formation, whereas longer-range Zn-Zn or framework correlation peaks become broadened or weakened[31]. This suggests that the periodic framework structure is transformed into an isotropic disordered network.

Figure 1 further summarizes this local preservation--long-range disorder structural feature. Single-crystal X-ray diffraction (XRD) indicates that certain coordination bonds in crystalline coordination frameworks become weakened before melting and may act as initiation sites for crystal-structure collapse and melting[32] [Figure 1A]. The differential scanning calorimetry (DSC) and dynamic mechanical analysis (DMA) results show that MOF glass formation is accompanied by clear melting, glass transition, and temperature-dependent viscosity changes, suggesting that these materials are not simply amorphized products but undergo an identifiable crystal-liquid-glass phase transition [Figure 1B]. Variable-temperature solid-state nuclear magnetic resonance (NMR) and molecular simulations reveal the presence of dynamically heterogeneous coordination environments during glass formation [Figure 1C]. Furthermore, reverse Monte Carlo (RMC) modeling, combined with pair distribution function (PDF), extended X-ray absorption fine structure (EXAFS), and magic-angle spinning nuclear magnetic resonance (MAS NMR) data, reconstructs the atomistic glass structure and further demonstrates that short-range coordination motifs can be retained within the glassy network, while medium- and long-range structures become significantly disordered [Figure 1D].

Compared with crystalline MOFs, such structural heterogeneity is particularly important because it introduces locally flexible coordination sites, that are difficult to achieve in ordered crystalline frameworks. The resulting disordered coordination networks therefore provide a structurally adaptive platform for ion transport, where local coordination fluctuations and dynamically rearrangeable environments may facilitate ion hopping and reduce migration barriers[33]. These characteristics increasingly suggest that the functional advantages of MOF glasses are not derived from preserving crystalline order, but rather from exploiting controlled disorder within coordination networks to enable emergent transport behaviors inaccessible in rigid crystalline MOFs.

Thermodynamic characteristics of MOF glasses

MOF glasses are the product of certain crystalline MOFs that undergo melting, quenching, and finally vitrify[34-36]. The thermodynamic characteristics of MOF glasses are fundamentally governed by the interplay between framework mobility, coordination dynamics, and temperature-dependent structural rearrangements during melting and vitrification. Unlike conventional inorganic glasses, MOF glasses

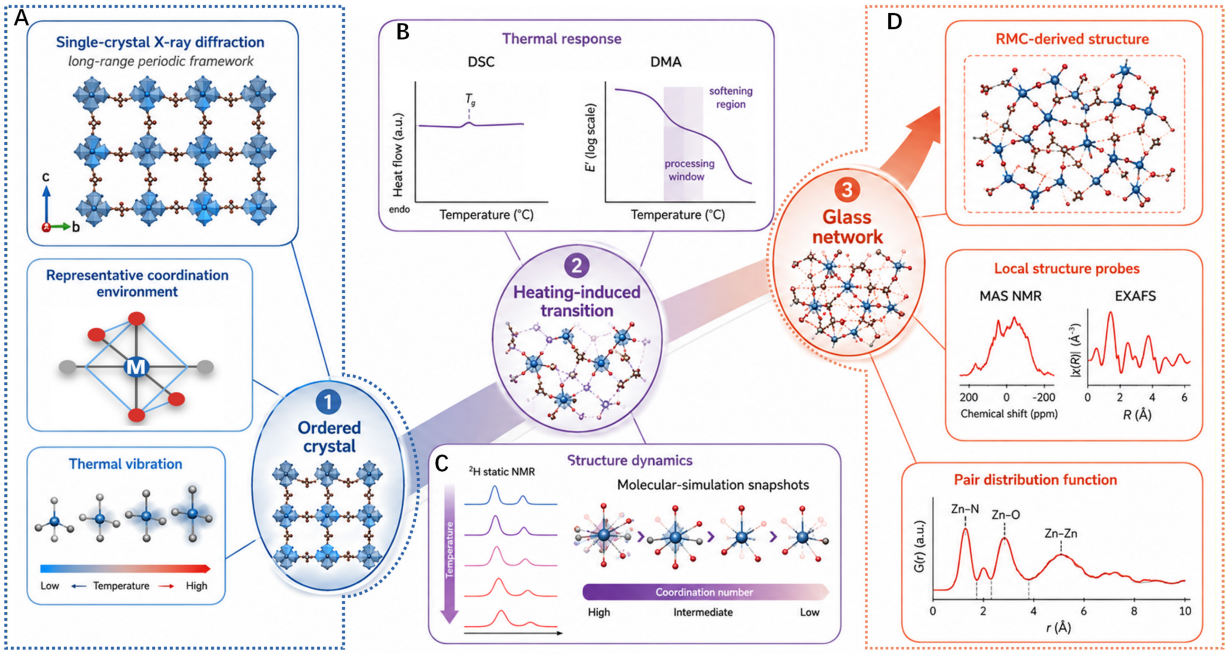

Figure 1. Selected characterizations of structures and phase transitions in MOFs. (A) Single-crystal XRD can determine the crystal structure, where mean atomic displacement retrieved from variable temperature measurements helps clarify the melting mechanism through Lindemann's rule; (B) Frequency-dependent dynamic mechanical analysis and DSC are used to determine thermal behavior, such as T_g; (C) Variable-temperature solid-state NMR and molecular simulation are examples of characterization methods that provide insight into structural dynamics; (D) RMC can provide atomistic modeling of the glass structure through the fitting of experimental data from PDF, EXAFS, and MAS NMR. DSC: Differential scanning calorimetry; DMA: dynamic mechanical analysis; MAS NMR: magic-angle spinning nuclear magnetic resonance; EXAFS: extended X-ray absorption fine structure; MOFs: metal-organic frameworks; XRD: X-ray diffraction; T_g: glass transition temperature; RMC: reverse Monte Carlo; PDF: pair distribution function.

originate from coordination networks in which metal-ligand bonds remain partially dynamic even in the liquid state, enabling a unique form of thermodynamic softening prior to complete structural collapse.

Among them, zeolitic imidazolate frameworks (ZIFs) family, especially ZIF-62, has received considerable interest due to its excellent glass-forming performance. Figure 2 illustrates the glass-forming process of ZIF-62[37]. Adopting similar structures to zeolites, the ZnN_4 tetrahedra in ZIF-62 replace SiO_4 tetrahedra and are linked by rigid organic ligands rather than less-constrained bridging oxygens [Figure 2A]. This zeolite-like tetrahedral topology reduces the angular constraints, and enables continuous framework reorganization upon heating, thereby fundamentally underpinning its ability to undergo vitrification prior to decomposition. The dominant prerequisite for MOF glass formation is the existence of a well-defined melting regime prior to framework decomposition, namely that the melting temperature (T_m) lies below the decomposition temperature (T_d), resulting in a sufficiently wide melting window[31] ($\Delta T = T_d - T_m$). Upon rapid cooling from the molten state, the disordered coordination network becomes kinetically arrested, suppressing crystal nucleation and growth, and yielding an amorphous glassy solid[37] [Figure 2B and C]. The melt-quench nature of MOF glasses allows shaping and device fabrication (e.g., hot imprinting and membrane processing). Compared with crystalline MOFs, bulk MOF glasses have been shown to possess mechanical robustness, which enables membrane fabrication and thermal processability, thereby enhancing their potential for device integration[22,38-41].

In the case of ZIF-4, molecular dynamics simulations provide mechanistic insight into the microscopic origin of MOF melting. As shown in Figure 3A, crystalline ZIF-4 transforms into a disordered melt at 1,500 K and can subsequently be quenched into a glassy state. The corresponding PDFs in Figure 3B show that the structural peaks broaden upon melting, indicating the loss of long-range order while short-range correlations remain partially preserved. Figure 3C further shows that the N-Zn-N bond-an-

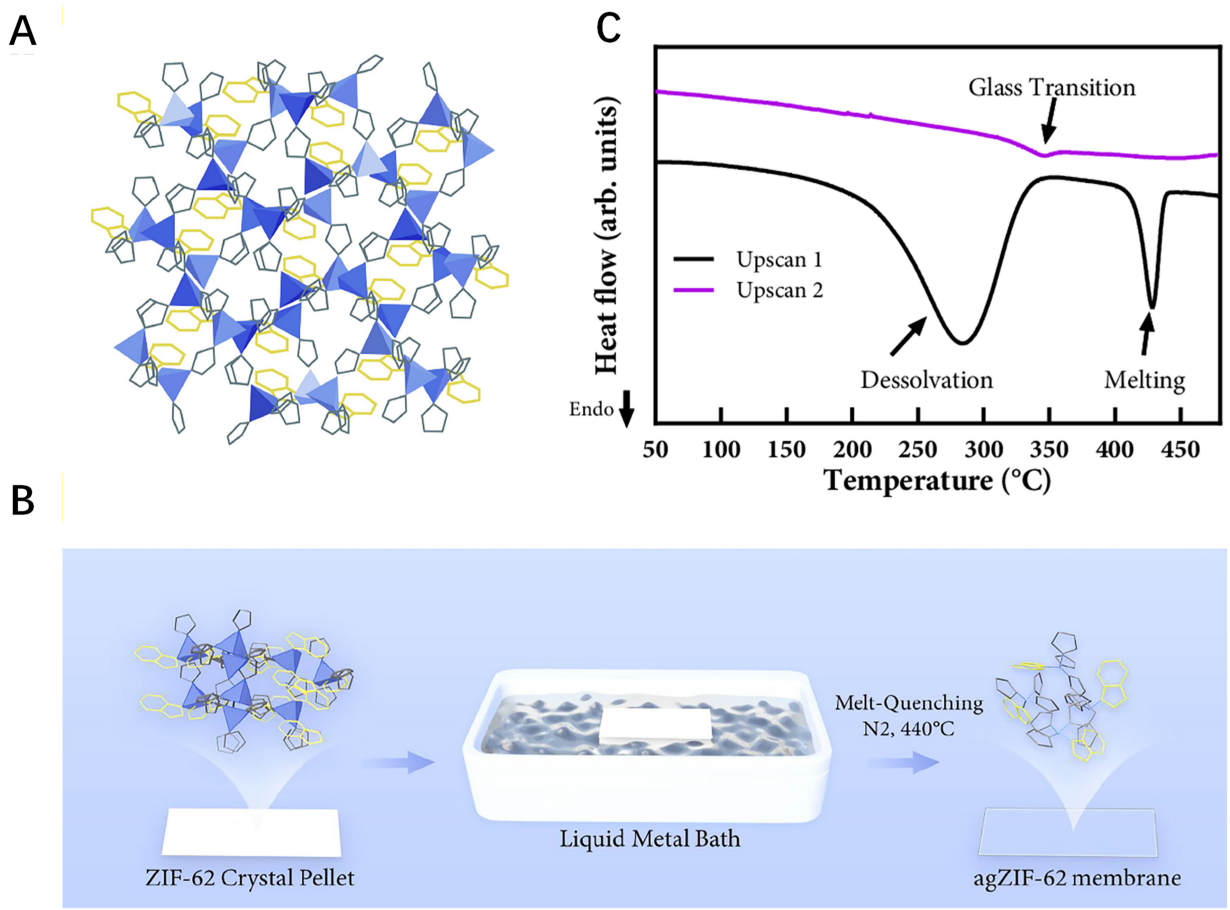

Figure 2. Structure and melt-quench glass formation of ZIF-62. (A) Zeolite-like tetrahedral framework of crystalline ZIF-62, consisting of tetrahedrally coordinated Zn^{2+} centers connected by imidazolate-based ligands; (B) Temperature-time pathway illustrating the melting, cooling and annealing process used to produce a_gZIF-62; (C) Flow chart of float glass fabrication method. ZIF-62 and the derived materials are shown in white. (A-C) Reproduced from reference[40], licensed under CC BY 4.0.

gle distribution becomes significantly broader in the molten state, suggesting distortion of the local ZnN_4 tetrahedral coordination environment. These changes indicate that ZIF-4 melting is associated with Zn-N coordination lability and local network rearrangement rather than complete collapse of the metal-ligand framework. Meanwhile, Figure 3D shows that the pore-size distribution becomes broader after melt-quenching, reflecting the formation of a more disordered glassy network. Overall, ZIF-4 melting produces a liquid-like disordered state in which local Zn-N connectivity and partial framework memory are retained, while medium- and long-range order is progressively lost[42].

Given the melting behavior of certain MOFs, the possible role of framework mobility in MOF-glass ion transport can be discussed with reference to soft matter electrolytes based on this broader principle: structural mobility and transient free-volume formation can influence ion migration in disordered solid electrolytes. Figure 4A shows the tensile deformation of polyethylene oxide (PEO)/$LiClO_4$ polymer electrolyte films, while both the in-plane and out-of-plane ionic conductivities increase with deformation/strain [Figure 4B]. This enhancement is attributed to cavitation-induced tiny voids, particularly in the amorphous regions of the semicrystalline polymer matrix [Figure 4C]. These voids increase free volume and may facilitate cooperative rearrangements of polymer chains, thereby improving ionic conductivity. In MOF-derived glass electrolytes, an analogous broad principle may apply, although through a distinct structural mechanism: glass-state framework mobility may promote ion migration through transient free-volume generation, local bond-angle fluctuations, and cooperative rearrangement of coordination motifs, rather than through

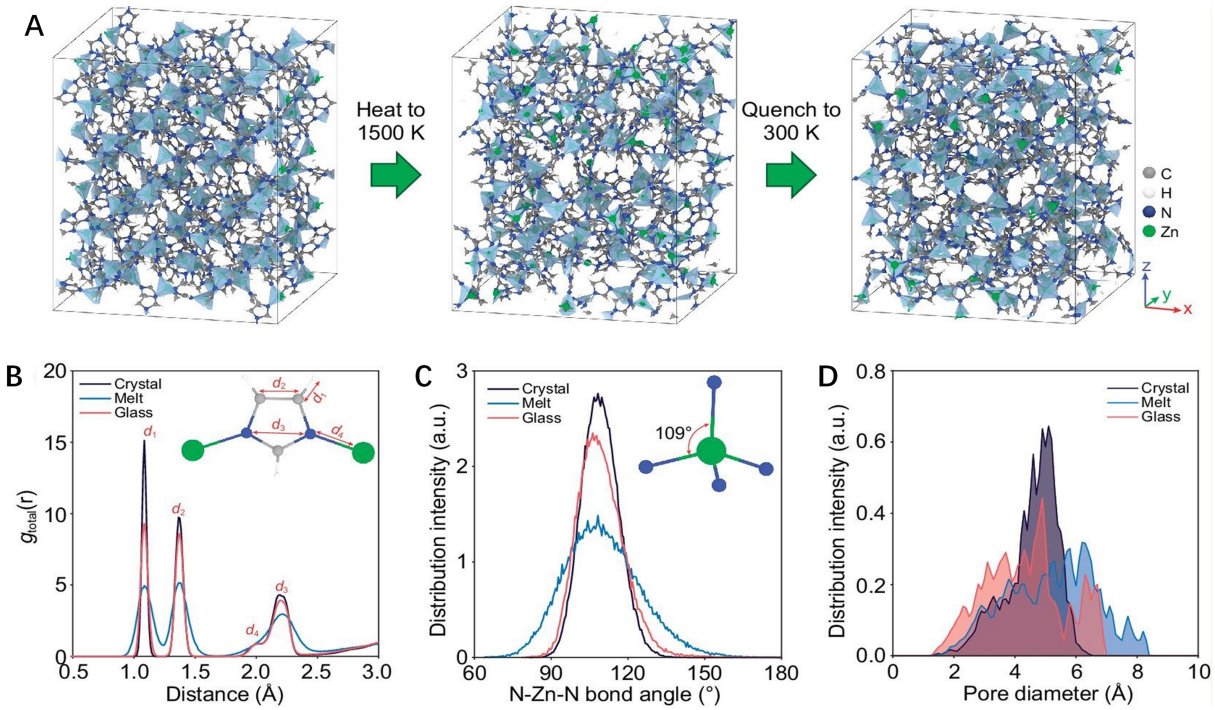

Figure 3. Melt-quenching simulation of ZIF-4 at zero pressure using deep learning force field. (A) Atomic configurations of ZIF-4 at different stages of the melt-quenching process, i.e., ZIF-4 crystal, molten ZIF-4 at 1,500 K, and quenched ZIF-4 glass at 300 K; (B-D) Calculated (B) pair distribution functions, (C) N-Zn-N bond angle distribution functions, and (D) pore size distribution of the ZIF-4 crystal, melt (at 1,500 K), and glass. (A-D) Reproduced from reference[42], licensed under CC BY 4.0.

polymer-chain segmental motion or a purely static hopping pathway.

In addition, it is important to note that MOF-glass conductivity is not governed by free volume or viscosity alone both of which are influenced by the vitrification process. Figure 5 further shows that, in Zn-H_nPO_4-based MOF glasses, changes in microdomain size and coordination-network connectivity alter bulk-phase viscosity but have only limited influence on ion conductivity. This suggests that local coordination chemistry, especially metal coordination number and ligand-based hopping-site density, can be more decisive than macroscopic viscosity. Therefore, MOF glasses should not be viewed simply as ordered crystals transformed into static amorphous solids, but as dynamically disordered yet partially connected coordination networks, in which framework mobility, free-volume evolution, thermodynamic relaxation, and local coordination motifs collectively regulate both vitrification and ion-transport properties.

Porosity and pore behavior in MOF glasses

Porosity and pore behavior in MOF glasses are fundamentally governed by the competition between structural densification during vitrification and the retention of accessible free volume inherited from the parent crystalline framework. Early studies on melt-quenched ZIF glasses showed that vitrification is often accompanied by substantial densification and loss of gas-accessible porosity[45]. For example, melt-quenched ZIF-4 was reported to form a nearly non-porous glass with a Brunauer-Emmett-Teller surface area below 5 $m^2 \cdot g^{-1}$, indicating severe collapse or contraction of the originally porous framework[35]. Subsequent positron annihilation lifetime spectroscopy studies further showed that a_gZIF-4 retains internal free volume, but much of this porosity is inaccessible to conventional gas sorption probes, highlighting the distinction between intrinsic free volume and gas-accessible porosity[46,47]. Similar reductions in accessible pore volume and surface area have also been observed in pressure-induced and mechanically amorphized ZIFs, suggesting that framework collapse, densification, and loss of long-range order commonly reduce the accessible porosity of amorphous MOF phases[48].

However, subsequent studies showed that porosity

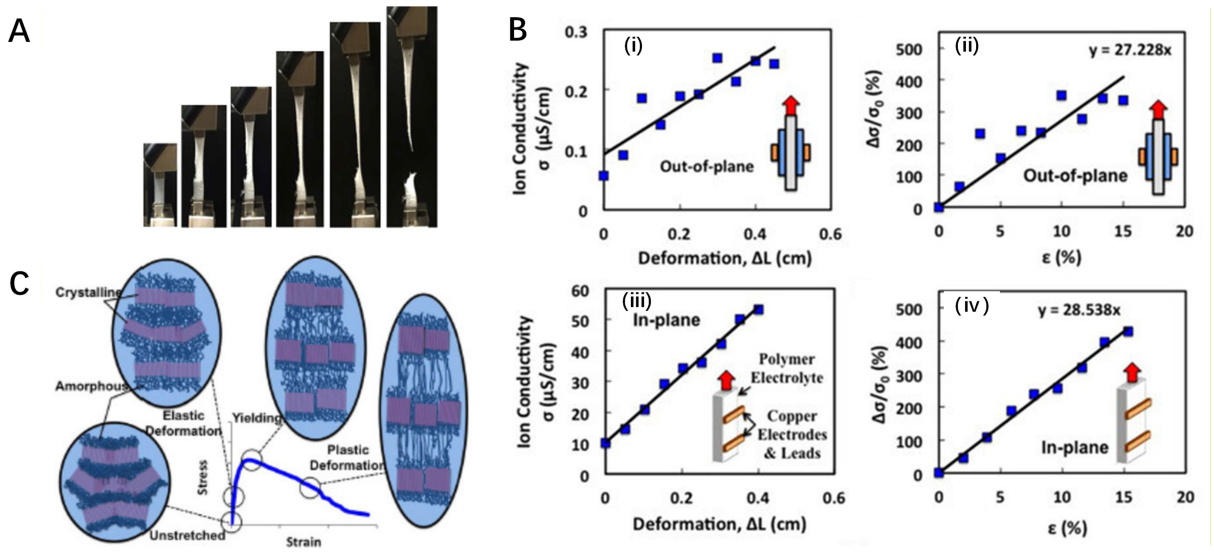

Figure 4. Framework mobility of soft matter electrolytes. (A) Photo images of PEO samples subjected to tensile deformation; (B) In-plane and out-of-plane ionic conductivities of PEO electrolyte (soft matter electrolyte) with respect to tensile deformation (in the direction of the red arrow). (i) Out-of-plane ionic conductivity *vs.* tensile deformation of PEO/Li salt film; (ii) Out-of-plane enhancement in ionic conductivity *vs.* tensile strain; (iii) In-plane ionic conductivity *vs.* tensile deformation; (iv) In-plane enhancement in ionic conductivity *vs.* tensile strain; (C) Depiction of semi-crystalline polymer microstructure at various stages of tensile deformation. (A-C) Reproduced from reference[43], licensed under CC BY 4.0. PEO: Polyethylene oxide.

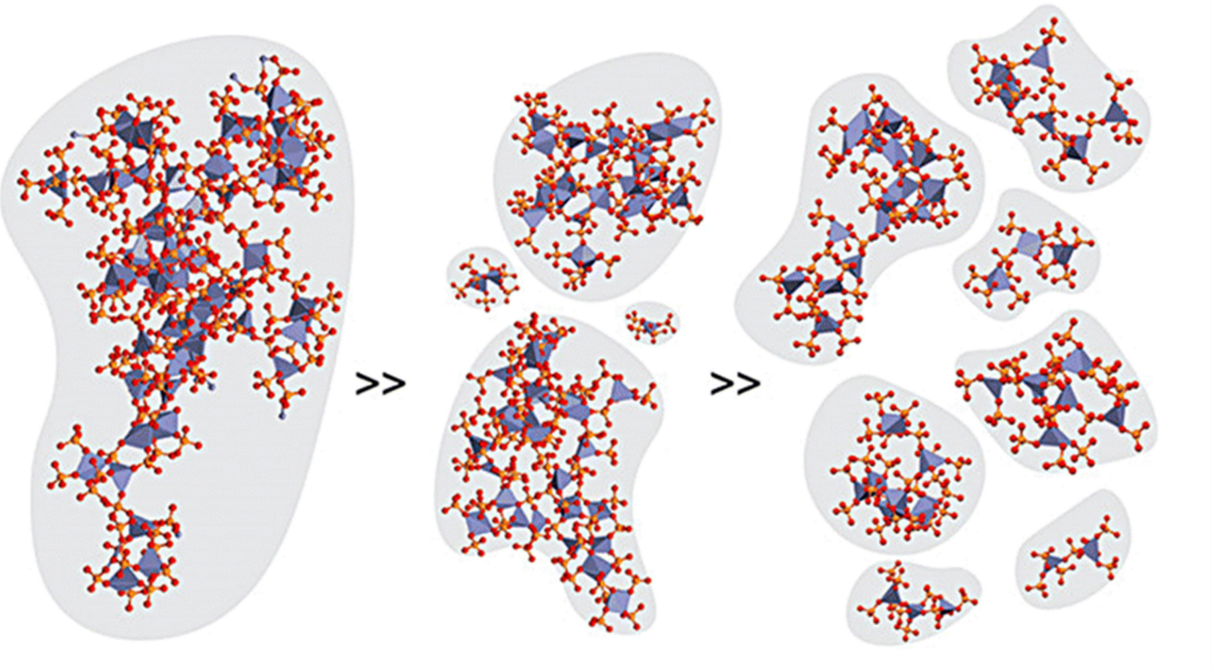

Figure 5. Comparable ion conductivities with change in average size of continuous networks. Zn-H_nPO_4 frameworks showed little change in ion conductivity with a change in the connectivity of the coordination networks. The gray areas provide visual aids to distinguish the increasingly disconnected coordination network. This figure is reproduced with permission from reference[44]. Copyright 2022, American Chemical Society.

in MOF glasses is not completely lost, but can evolve into a partially retained and dynamically heterogeneous microporous network. As Figure 6 shows, porous glasses derived from ZIF-76 and ZIF-76-mbIm demonstrate that bulky benzimidazolate-based linkers can inhibit dense packing in the

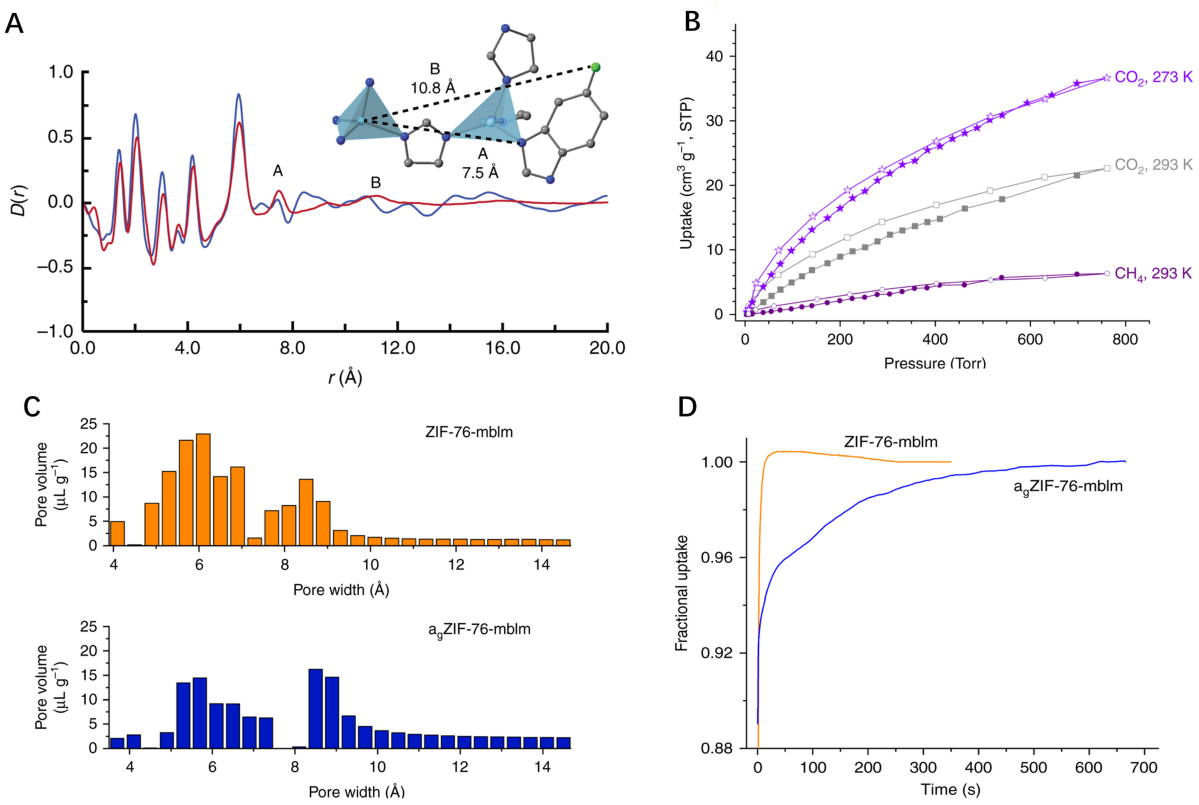

Figure 6. Structural retention and gas-accessible microporosity in ZIF-derived glasses. (A) ZIF-76 pair distribution function D(r). Inset shows medium-range order. Zn light blue, Cl green, C grey, N dark blue, H omitted for clarity; (B) Adsorption isotherms of a_gZIF-76-mbIm (filled symbols = adsorption, empty symbols = desorption); (C) Pore size distributions as determined by a NLDFT method from CO_2 adsorption isotherms at 273 K; (D) Time-dependent CO_2 uptake profiles at 273 K at a pressure of 5 Torr. (A-D) Reproduced from reference[49], licensed under CC BY 4.0. NLDFT: Non-local density functional theory.

liquid state and help preserve free volume after vitrification. The PDFs of crystalline and glassy samples remain nearly identical below ~6 Å, indicating that local C-C/C-N and Zn-N correlations are preserved, while the remaining features beyond 6 Å, especially around 7.5 and 10.8 Å, further suggest retained medium-range Zn-imidazolate-Zn-benzimidazolate connectivity in the glass state [Figure 6A]. This retained structure is confirmed to lead to functional pore accessibility, as a_gZIF-76-mbIm reversibly adsorbs CO_2 and CH_4 [Figure 6B]. Meanwhile, vitrification contracts the pore-size distribution but still preserves microporous voids, consistent with positron annihilation lifetime spectroscopy (PALS)-detected pores of ~4.8 and 7.2 Å [Figure 6C]. But the slower CO_2 uptake in the glass indicates there are more tortuous and constricted diffusion pathways in glass state [Figure 6D]. Together, these results suggest that transport accessibility in MOF glasses arises from interconnected disordered cavities rather than conventional crystalline pore channels.

Recent studies have therefore increasingly explored pore engineering strategies to overcome vitrification-induced densification, including linker steric modulation, mixed-linker design, crystal-glass composites, and porogen-assisted approaches inspired by traditional porous glass fabrication[50]. In particular, porogen strategies involving thermally decomposable salts, polymers, or sacrificial fillers have been proposed as promising routes for introducing hierarchical porosity and tunable pore architectures into MOF glasses. The introduction of hierarchical porosity may be especially important because ion and gas transport in dense glassy networks is frequently limited by diffusion bottlenecks and restricted pore interconnectivity. Moreover, the macroscopically grain-boundary-free nature of MOF glasses provides an additional advantage over crystalline MOFs, as continuous isotropic transport pathways may emerge when pore connectivity is successfully retained. Consequently, pore behavior in MOF glasses should not be interpreted simply as a

loss of crystallinity-induced porosity, but rather as the evolution of adaptive disordered free-volume networks whose accessibility, connectivity, and transport functionality can potentially be engineered through controlled liquid-state structural design and vitrification processes.

ALKALI METAL CATIONS TRANSPORT BEHAVIORS AND MECHANISMS IN MOF GLASSES

From a solid-state ionic perspective, alkali-ion transport in MOF glasses can be understood through broader concepts such as disorder-assisted migration, frustrated ion environments, and concerted ion motion. In fast SSEs, disorder and mobile-ion frustration can flatten the migration energy landscape, while concerted migration allows neighboring ions to move cooperatively and reduce activation barriers[51]. These concepts are highly relevant to MOF glasses because their disordered coordination networks, flexible metal-ligand bonds, and fluctuating free-volume domains may similarly lower ion-migration barriers.

Li^+ and Na^+ transport behaviors and mechanisms in MOF glasses

For alkali metal cations, transport in MOF glasses is not simply governed by rigid pore diffusion[52]. Instead, it is strongly affected by the coupled effects of free volume, coordination disorder, linker dynamics, and local ion-framework interactions.

The recent ZIF-62 glass electrolyte study showed that Li^+ migration in glassy ZIF-62 occurs through a "relay-race" mechanism, where Li^+ is dynamically delivered between N sites from imidazole and benzimidazole ligands. Compared with crystalline ZIF-62, the glass phase provides a larger Li^+ migration space, higher calculated Li^+ diffusivity, and more continuous homogeneous transport channels. In crystalline ZIF-62, Li^+ motion is confined to localized regions, whereas glassy ZIF-62 provides a larger spatial distribution for Li^+ migration [Figure 7A and B]. The mean square displacement (MSD) analysis further shows that the calculated Li^+ diffusivity in glassy ZIF-62 is 3.97×10^{-9} $m^2 \cdot s^{-1}$, which is higher than that in crystalline ZIF-62 (1.43×10^{-9} $m^2 \cdot s^{-1}$) [Figure 7C]. Within the same simulation time frame, the Li^+ migration distance is approximately 1.49 Å in crystalline ZIF-62, but increases to approximately 3.92 Å in glassy ZIF-62, indicating faster Li^+ migration and a more open transport space in the glassy phase [Figure 7D and E]. In addition, Li^+ trajectories in crystalline ZIF-62 are relatively localized and mainly distributed around N species, whereas in glassy ZIF-62, the Li^+ trajectories become more continuous along N atoms [Figure 7F and G]. The radial distribution function further reveals that the Li-N distance increases from approximately 2.14 Å in the crystalline phase to 2.22 Å in the glassy phase. This longer Li-N distance suggests weaker interactions between Li^+ and N sites in glassy ZIF-62, making Li^+ easier to detach from one N site and migrate to another [Figure 7H]. Consistently, the Li^+ migration activation energy calculated from the Arrhenius relationship was 0.17 eV for glassy ZIF-62 quasi-solid-state electrolyte (GZ-62-QSSE), lower than that of crystalline ZIF-62 quasi-solid-state electrolyte (CZ-62-QSSE), 0.20 eV. In contrast, the binding energy between Li^+ and GZ-62-QSSE was only 0.21 eV, markedly lower than that between Li^+ and CZ-62-QSSE, 2.91 eV[53]. These results demonstrate that incompletely coordinated Zn^{2+} sites and distorted coordination environments generated by vitrification can immobilize anions, weaken Li^+ binding, and thereby promote Li^+ migration.

Another important Li^+-related mechanism is modifier-induced network depolymerization. In lithium benzimidazolate-modified ZIF-62 glasses, Li(bIm) acts as a compatible glass modifier. Rather than merely occupying the residual pores, Li(bIm) becomes incorporated into the disordered glass network and disrupts the original Zn-Im/bIm-Zn connectivity, generating non-Zn-bridging linker environments and partially depolymerizing the framework. This structural modification lowers the glass-transition temperature and increases the configurational freedom of the network. These results suggest that Li^+ can influence ion transport not only as a potential mobile charge carrier but also by modifying the local coordination network and increasing structural flexibility[54].

Porosity and free volume also play a central role. MOF glass formation often causes partial pore collapse, which may impede Li^+ transport by generating dead-end pathways. Therefore, alkali-ion transport in MOF glasses should be understood as a coupled structure-dynamics process. The most important mechanisms include: N-site-assisted

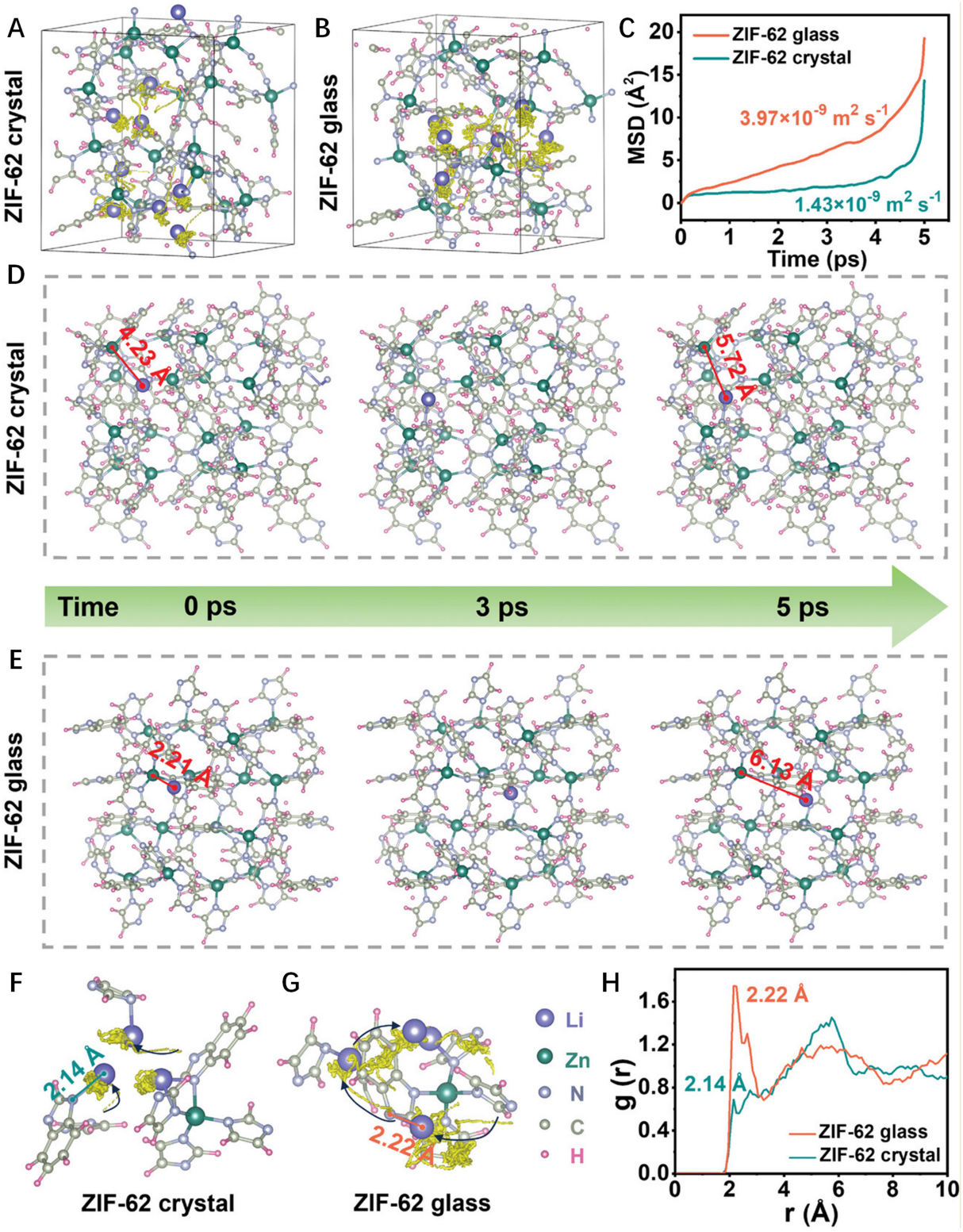

Figure 7. Li^+ migration mechanism in crystalline and glassy ZIF-62. Atom position distribution of Li in (A) ZIF-62 crystal and (B) ZIF-62 glass; (C) Li MSD in crystalline and glassy ZIF-62 during 5 ps; (D and E) Structural snapshots of Li^+ migration in ZIF-62 crystal and ZIF-62 glass from AIMD simulations. Movement trajectories of Li element in (F) ZIF-62 crystal and (G) ZIF-62 glass; (H) RDF of Li-N in ZIF-62 crystal and ZIF-62 glass. The yellow curves in (A), (B), (F) and (G) represent the movement trajectories of Li ions. This figure is quoted with permission from reference[53]. Copyright 2025, Wiley-VCH GmbH. RDF: Radial distribution function; AIMD: ab initio molecular dynamics.

hopping, free-volume-mediated diffusion, modifier-induced network depolymerization, coordination disorder, and glass-dynamics-assisted ion migration. Future MOF-glass-based SSEs may be ration-

ally designed by combining alkali salt incorporation, defect engineering, pore accessibility control, and thermodynamic softening to create continuous, isotropic, and dynamically adaptive ion-transport networks[26].

Na^+ and K^+ transport in MOF glasses: an emerging but underdeveloped direction

In disordered or amorphous solid electrolytes, Na^+ transport is strongly affected by the topology of the local free-volume network, the distribution of transient coordination sites, and the connectivity of ion-hopping pathways. Recent studies on amorphous and nanocrystalline Na-Y-Zr-Cl halide electrolytes showed that the introduction of amorphous domains can enhance Na^+ conductivity by reducing grain-size-related transport barriers and generating more continuous ion-transport pathways[55]. Similarly, molecular-dynamics studies on amorphous alkali oxyhalides indicate that alkali-ion migration is governed by local anion coordination, residence time near framework-forming units, and ion-ion correlation effects rather than by rigid crystallographic channels alone[56]. These findings suggest that, in MOF glasses, Na^+ migration should be understood as transport through a dynamically connected disordered free-volume network, where both bottleneck size and the flexibility of local coordination environments are critical.

MOF-based Na^+ solid electrolytes further highlight the importance of pore size and channel chemistry. Nozari *et al.* introduced the sodium-salt-containing ionic liquid ($Na_{0.1}EMIM_{0.9}$) (Na0.1[1-ethyl-3-methylimidazolium]0.9) bis(trifluoromethanesulfonyl)imide (TFSI) into ZIF-8 and demonstrated that MOF-ionic liquid host-guest interactions can promote high Na^+ conductivity, while structural disorder improves the stability of the composite electrolyte[57]. In MOF-74 systems, the one-dimensional hexagonal channels and open metal sites provide larger ion-conducting pathways and sites for anion immobilization. For example, Na/Mg-MOF-74 exhibited an ionic conductivity of 8.53×10^{-4} S·cm^{-1} at 70 °C, which was attributed to its stable ion-conducting channels and exposed Mg^{2+} sites[58]. Similarly, Na[EMIm][TFSI]@Zn-MOF-74 reached 5×10^{-4} S·cm^{-1} at room temperature and enabled stable sodium plating for over 100 h[59].

Therefore, the design principles established for Li^+ conducting MOF glasses cannot be directly transferred to Na^+ systems. Because Na^+ has a larger ionic radius and different coordination preferences, Na^+ conductors generally require wider bottlenecks, larger accessible free volume, weaker ion-framework binding, and more continuous percolated pathways. However, current studies remain limited: most Na^+ MOF electrolytes rely on crystalline MOFs or ionic-liquid-filled composites, while direct evidence for Na^+ migration in genuine MOF glass networks is still scarce. Future work should therefore combine structural characterization, ion-dynamics simulations, and electrochemical measurements to clarify how glass topology, free-volume distribution, and anion immobilization jointly regulate Na^+ transport.

Compared with Li^+ transport, K^+ conduction in MOF glasses remains largely unexplored. To date, most reported alkali-metal-ion-conducting MOF glasses and MOF-glass-containing electrolytes have focused on Li^+ transport, as exemplified by glassy ZIF-based quasi-solid-state electrolytes for lithium-metal batteries[53]. In contrast, K^+ conducting MOF systems reported so far are mainly based on crystalline single-ion-conducting frameworks or MOF/polymer composite electrolytes rather than melt-quenched MOF glasses[60,61]. For example, MOF-808-SO_3K has been reported as a single potassium-ion conducting crystalline MOF, in which immobilized sulfonate groups provide fixed anionic sites and K^+ serves as the mobile charge carrier[61]. More recently, MOF-containing composite polymer electrolytes have also been developed for solid-state potassium batteries, where UiO-66 is incorporated into a poly(vinylidene fluoride-co-hexafluoropropylene) (PVDF-HFP)-based polymer matrix to enhance mechanical stability, increase polymer disorder, and provide K^+ migration channels[60]. These examples demonstrate the feasibility of K^+ transport in MOF-based electrolyte systems, but they also highlight that the structure-transport relationships established in crystalline MOFs or MOF/polymer composites cannot be directly transferred to MOF glasses.

The scarcity of K^+ conducting MOF glasses likely arises from several coupled challenges. K^+ has a larger ionic radius and lower charge density than Li^+, making its transport more sensitive to pore aperture, free-volume size, and the availability of weakly coor-

dinating sites[62,63]. Besides, many glass-forming MOFs are charge-neutral frameworks without intrinsic fixed anionic groups; therefore, K^+ transport generally requires the incorporation of external potassium salts, ionic liquids, or framework-bound anionic functionalities[54]. The preparation of homogeneous K^+ containing MOF glasses is also synthetically challenging, as the potassium salts may crystallize, phase-separate, or decompose during high-temperature melting and quenching. This issue is particularly relevant because MOF glasses are generally produced by heating/melting followed by rapid quenching[64-66]. These factors explain why K^+ conduction in MOF glasses remains an important research gap and suggest that future studies should focus on designing glass-forming frameworks with sufficiently large and connected free-volume elements, introducing fixed anionic sites or weakly coordinating ligands, and suppressing salt crystallization to enable continuous K^+ transport.

STRATEGIES FOR DEVELOPING ION-CONDUCTING MOF GLASSES

A major challenge that many MOFs suffer from is their melting behavior. They either cannot melt or their melting points exceed their T_d, which greatly hinder the formation of dense glass or amorphous phases, hence impeding their applications in ion transportation. Another challenge for MOF glass conductors is that their ionic conductivity is still relatively low (ionic conductivity ~10^{-7}-10^{-3} S·cm^{-1}) compared with those of current oxide and sulfide electrolytes mentioned in Section "INTRODUCTION"[28,29,38]. These challenges have led to the relatively limited number of studies on ionic-conducting MOF glasses.

Although significant progress has been made through several strategies, including additive modulation, transient flux, and coordination environment engineering, these approaches have largely been developed independently, with limited integration aimed at simultaneously facilitating vitrification and enhancing ionic conductivity. As a result, a critical knowledge gap persists: how can thermodynamic softening and ion-transport engineering be mechanistically integrated rather than empirically combined?

Building on the insights about strategies mentioned above, we propose a new viewpoint that molten salts can act as dual-function flux-network modifiers, simultaneously lowering the effective melting threshold and pre-structuring the resulting glass to facilitate ion conduction. We outline the mechanistic basis of this coupling, discuss emerging opportunities for rational materials design, and identify key challenges toward realizing high-performance hybrid MOF glass electrolytes.

Additive modulation strategies in developing MOF glass ionic conductor

Thermodynamic modulation toward accessible MOF vitrification

From a thermodynamic perspective, the key challenge in accessing MOF glasses lies in enabling framework reorganization to occur prior to decomposition. Introducing additives into MOF glasses can be achieved by chemical substitution, guest incorporation, and topology engineering. They provide an intrinsic means of thermodynamic modulation by directly altering local coordination strength and network rigidity. The additives refer to the introduction of foreign atoms, ions or molecules (impurities) into crystals or glass, which have a relatively low concentration but can alter the chemical environment and electronic structure of the material.

In porous carbon synthesis, the dissolution-rearrangement of ZIF-8 in a $MgCl_2·6H_2O$ molten salt medium below 300 °C demonstrates that a salt environment can substantially lower the energetic threshold for structural transformation, compared to conventional solid-state pyrolysis of ZIF-8, which typically requires more than 700 °C to induce framework collapse and carbonization[67]. This observation highlights the general capability of molten salts to unlock low-temperature structural reorganization pathways and provides a conceptual basis for extending such strategies to MOF systems more broadly. Together, these results highlight the general role of molten salts in lowering both energetic and kinetic barriers for MOF melting and vitrification. Recent work by Cao *et al.* directly demonstrated that co-melting heterocycle-based benzimidazolium halide salts (Cl^-, Br^-, I^-) with ZIF crystals enables framework melting at temperatures below 300 °C and yields exceptionally low glass transition temperatures (T_g < 150 °C)[68]. Figure 8 shows that, during

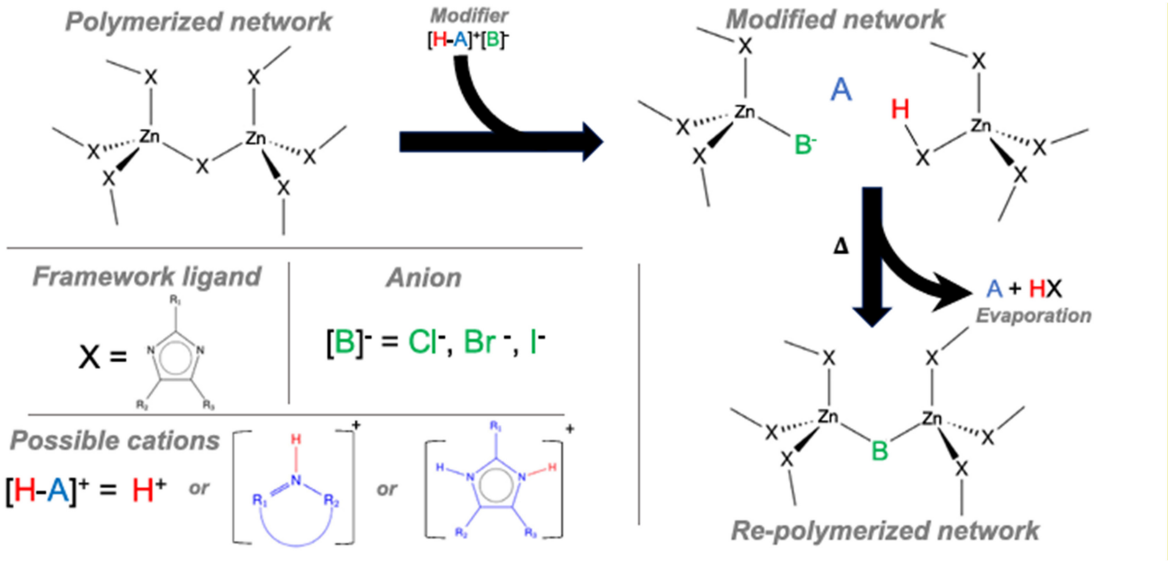

Figure 8. Mechanism of modification for ZIF glasses using benzimidazolium halide salts. This figure is quoted with permission from reference[68], licensed under CC BY 4.0.

thermal treatment, halide anions coordinate with Zn centers while proton exchange from the cation modifies the local coordination environment, leading to the formation of mixed-linker configurations. This process enables continuous structural reconstruction of the framework. Upon further heating, partial evaporation of linker species may occur, followed by repolymerization into a modified network with increased Zn-halide connectivity.

Molten inorganic salts can directly interact with metal-ligand coordination environments during thermal processing, enhancing mass transport, thereby enabling controlled framework reconstruction and pore evolution[69]. Beyond this, they also act as intrinsic sources of mobile charge carriers, introducing ions such as Li^+ into the evolving network and thereby enabling ionic conduction within the resulting glass.

Guest modulating strategies demonstrate that thermodynamic accessibility of MOF glasses can be rationally engineered. Nevertheless, these approaches primarily regulate when and how melting occurs, rather than the functional properties of the resulting glasses. Consequently, thermodynamic modulation alone remains insufficient for achieving high-performance MOF glass electrolytes, motivating parallel efforts in transport regulation discussed in the following section.

Conductivity enhancement of MOF glasses

Beyond thermodynamic accessibility, achieving practically relevant ionic conductivity constitutes an equally critical challenge for MOF-based solid electrolytes, including both crystalline MOFs and MOF glasses. This section focuses specifically on strategies for enhancing ionic transport in MOFs and MOF glasses, where the framework serves as a mechanically rigid host for mobile charge carriers introduced via guests[13,70,71]. Unlike thermodynamic modulation, these approaches target carrier concentration, mobility, and percolation pathways, and are often developed independently of melting or vitrification considerations.

Early studies predominantly focused on intrinsic ionic conduction, especially proton transport mediated by hydrogen-bonded networks, which are usually formed by acidic ligands, coordinated water molecules, or guest acids[72,73]. In such proton-conducting MOFs, conductivities in the range of 10^{-4}-10^{-2} $S \cdot cm^{-1}$ have been reported under high humidity (RH > 90%) and moderate temperatures (60-90 °C)[74-76]. However, the strong dependence on water content and the instability of hydrated structures significantly limit long-term operation and high-temperature applicability[77].

To address these challenges, increasing attention has been directed toward extrinsic ionic conduction, in

which MOFs serve as rigid scaffolds hosting mobile ionic species introduced via guest salts or ionic liquids[78]. Ionic liquid-infiltrated MOFs (IL@MOFs) often show enhanced ion transport, with conductivities reaching 10^{-4} S·cm^{-1} at room temperature, while offering favorable thermal robustness compared with conventional polymer-based electrolytes[57,79,80]. Table 1 summarizes previous research on conducting MOFs and MOFs-based electrolytes systems.

Ionic conduction in IL@MOF systems originates from the synergistic interplay between confined ionic liquids and the host framework[96]. As Figure 9 shows, the ionic liquid provides a reservoir of mobile charge carriers, while nanoscale confinement within MOF pores alters ion coordination and suppresses ion pairing, thereby increasing the population of free charge carriers. Meanwhile, the MOF framework actively modulates ion transport through interfacial interactions and steric constraints. Specifically, framework sites can immobilize or slow down anions via coordination or adsorption, resulting in enhanced cation transference. In addition, the well-defined pore architecture establishes continuous ion-conduction pathways and reduces tortuosity for ion migration. As a result, ionic transport in IL@MOFs is governed by a combination of confinement-enhanced ion dissociation, framework-mediated ion selectivity, and percolated transport pathways within the confined liquid phase.

While substantial progress has been made in enhancing ionic conductivity through guest incorporation and framework disorder, these strategies frequently rely on elevated operating temperatures or liquid-like transport behavior to achieve high conductivities. Consequently, ionic conductivity enhancement has remained largely decoupled from thermodynamic accessibility and structural stability under device-relevant operating conditions, underscoring the need for integrated approaches that simultaneously address transport and thermodynamic constraints.

Transient flux strategies in developing MOF glass ionic conductor

Different from additive modulation, transient flux-assisted processing relies on the presence of an external molten medium during heating, which facilitates mass transport and framework rearrangement without necessarily becoming a permanent component of the final glass[97]. In MOF systems, meltable frameworks phases can act as transient fluxes, enabling the co-melting of otherwise non-meltable MOFs and expanding the accessible vitrification window. By lowering kinetic barriers associated with solid-state diffusion and coordination rearrangement, flux-assisted pathways allow melting to occur at temperatures below the intrinsic decomposition threshold. Previous research used meltable ZIF-62 to dissolve non-fusible ZIF-8 in a liquid phase effectively lowering the overall melting threshold, and the whole composite achieved co-melting at 430-450 °C[98] [Figure 10A and B]. Flux melting also provides a promising pathway for constructing ion-conductive MOF glasses through the formation of newly accessible disordered pore networks. Although the original crystalline pore structure of ZIF-8 collapses during vitrification, the incorporation of ZIF-8 into the liquid ZIF-62 matrix disrupts dense liquid-state packing and generates a less compact disordered framework with enlarged pore-limiting apertures and enhanced free volume [Figure 10C-E]. The resulting flux-melted glass exhibits significantly improved H_2 accessibility and larger transport apertures compared with pure a_gZIF-62, indicating the emergence of more continuous and accessible diffusion pathways within the disordered coordination network [Figure 10F]. Such dynamically disordered pore environments may be particularly beneficial for ionic transport because they can reduce steric constraints and facilitate ion hopping through interconnected free-volume domains. In contrast to rigid crystalline pore channels, these isotropic disordered networks may also provide macroscopically grain-boundary-free transport pathways and adaptable coordination environments capable of accommodating alkali ions during migration. Therefore, flux-mediated pore restructuring not only expands the vitrification accessibility of non-melting MOFs, but also suggests a viable strategy for engineering transport-accessible MOF glasses with potential ionic conduction functionality.

Coordination-environment engineering strategies

At a higher structural level, topology and network engineering offer a powerful means of thermodynamic regulation by modifying the global constraint landscape of MOFs. Reductions in framework connectivity, changes in network topology, or cooperative interactions with confined guests can increase configurational freedom and defect density,

Table 1. Representative MOF-glass, non-ZIF MOF, and IL@MOF ion-conducting systems with material-level conductive phase, performance, and limitations

Category	Specific material	Conductive phase/transport pathway	Ion	Performance	Comparative strength	Limitations/trade-offs	Suggested reference
ZIF-derived MOF electrolyte	Glassy ZIF-4 QSSE	Glassy ZIF-4 network with lean Li salt/solvent phase confined in the glass-derived framework	Li^+	1.61×10^{-4} S·cm^{-1} at 30 °C		Quasi-solid-state rather than fully dry single-phase glass; residual liquid/solvent contribution should be stated clearly	[27]
	ZIF-62 glass in PEO-LiTFSI/IL electrolyte	Disordered ZIF-62 glass as isotropic filler; Li^+ mainly transported through IL-rich phase and improved filler/electrolyte wetting	Li^+	2.41×10^{-4} S·cm^{-1} at 30 °C; 9.46×10^{-4} S·cm^{-1} at 70 °C		Composite effect, not intrinsic dry MOF-glass conduction; performance depends on polymer, IL and filler loading	[81]
	Vitrified MOF composite (glassy ZIF-62) electrolyte (PGZ)	Vitrified MOF-derived composite framework with polymer/gel electrolyte phase enabling Li^+ migration	Li^+	~6.3×10^{-4} S·cm^{-1}	Relatively high room-temperature ionic conductivity, stable glassy state improves processability and ion transport	Composite rather than single-component glass; the exact conductive phase must be separated from the MOF-glass scaffold	[82]
	Porous ZIF-62 glass gelled polymer electrolyte (PMG-GPE)	Top-down carved porous MOF glass with 3D interconnected graded-aperture channels; gel/polymer phase supplies Li salt and continuous ion medium	Li^+	Up to ~1.9×10^{-3} S·cm^{-1} at RT		Gelled polymer/composite electrolyte; conductivity cannot be attributed solely to dry MOF glass	[79]
	Boundary-free ZIF-62 glass SSE for Li-O_2 batteries	Continuous MOF-glass phase designed to remove grain boundaries and support Li+ transport/interface stability	Li^+	~5×10^{-4} S·cm^{-1} at 20 °C		Cell chemistry is Li-O_2-specific; synthesis and oxygen-electrolyte interface may not directly transfer to Li-ion or Na-ion cells	[25]
	NaTFSI/[EMIM][TFSI]@ZIF-8	Superionic sodium IL phase confined in/disordered by ZIF-8; structural disorder improves stability and transport	Na^+	~6×10^{-3} S·cm^{-1} at RT	Very high Na^+ conductivity; key benchmark for IL-impregnated MOF sodium conductors	Non-glassy phase, Main conduction comes from IL-rich phase; mixed-ion contribution and liquid containment must be discussed	[57]
Crystalline carboxylate MOF	MOF-808-based solid-state electrolyte	MOF-808 host/framework combined with Li salt phase; open Zr-cluster chemistry may assist salt dissociation and Li^+ migration	Li^+	3.08×10^{-3} S·cm^{-1} at 25 °C	High room-temperature ionic conductivity, combined with a high lithium-ion transference number and good cycling stability	MOF-808 itself is not an intrinsic fast Li^+ conductor, and its performance mainly depends on confined liquid/quasi-liquid electrolyte species within its pores	[83]
	MOF-808-SO_3K wetted with propylene carbonate	Single-ion K^+ conductor: tethered sulfonate anions immobilize countercharge; PC wets pellet and assists K^+ mobility	K^+	3.1×10^{-5} S·cm^{-1} at 303 K; K^+ transference number 0.76	Immobilized sulfonate anions enable single K^+ conduction with a high K^+ transference number	Lower conductivity than many IL@MOF Li/Na systems; solvent-wetted pellet rather than dry glass; particulate crystalline nature may limit practical solid-state battery applications	[61]

	[BMP][TFSI]@UiO-66	Confined ionic liquid in UiO-66 pores; ionic liquid phase dominates conduction	Li^+	3.3×10^{-4} S·cm^{-1} at RT	Competitive structural design; the higher packing density enhances ion transport	Liquid-containing system; possible mixed cation/anion transport and leakage/plasticization issues	[84]
	[EMIM][TFSI]@UiO-67	Confined EMIM-TFSI phase in larger-pore UiO-67; Li^+ transport assisted by IL mobility	Li^+	1.0×10^{-4} S·cm^{-1} at RT	Shows pore-size/linker extension effect relative to UiO-66-type hosts	IL phase can dominate conductivity; larger pores may reduce confinement and ion selectivity	[85]
	[EMIM][TFSI]@MOF-525(Cu)	Ionic liquid confined in crystalline MOF-525(Cu) pores, with nanowetted interfaces improving electrode contact	Li^+	3.0 × 10-4 S·cm^{-1} at RT	High RT conductivity for an IL@MOF electrolyte; nanowetted interfaces improve Li-metal contact and reduce interfacial resistance	Not MOF glass; conductivity mainly arises from IL phase rather than intrinsic MOF framework; apparent conductivity may be affected by excess surface IL; Li^+ transference and IL retention should be considered	[86]
	[BMP][TFSI]@UiO-66	Li-containing ionic liquid confined in UiO-66 pores	Li^+	3.3×10^{-4} S·cm^{-1} atRT	High RT conductivity for crystalline IL@MOF electrolyte; nanostructured UiO-66/Li-IL improves bulk Li^+ transport and electrode/electrolyte interfacial contact	Not intrinsic MOF or MOF-glass conduction; conductivity mainly depends on confined Li-IL phase; possible mixed-ion transport from IL; long-term IL retention and surface/excess IL effects should be considered	[87]
Crystalline carboxylate MOF + IL	[EMIM][TFSI]+ UiO-66@UiO-67	Li-containing ionic liquid hosted in UiO-66@UiO-67 nanopores	Li^+	2.1×10^{-4} S·cm^{-1}	Core-shell MOF-in-MOF combines high IL uptake from UiO-67 shell and ion-selective confinement from UiO-66 core; higher conductivity and Li^+ transport than homogeneous UiO-66/Li-IL or UiO-67/Li-IL hosts	Not intrinsic MOF or MOF-glass conduction; conductivity mainly arises from Li-IL phase; mixed-ion transport and IL retention/excess IL effects should be considered; core-shell synthesis is more complex than single-MOF hosts	[88]
	MIL-121/Li + [EMIM][TFSI]	Apparent conduction mainly from EMIM-TFSI-rich external/interparticle phase; Li^+ in MIL-121/Li remains largely immobile	Li^+	5.0×10^{-4} S·cm^{-1} at 30 °C for MIL-121/Li + 23 wt% EMIM-TFSI	Stable confinement of ionic liquid to enhance Li^+ transport	Not intrinsic MOF conduction; dry MIL-121/Li is nearly insulating; IL may not enter pores effectively; apparent conductivity can be dominated by external IL	[89]
	NaTFSI in Bmpyr-TFSI@UiO-66	Na salt dissolved in pyrrolidinium-TFSI IL confined by sulfonated/UiO-66-type MOF host	Na^+	3.6×10^{-4} S·cm^{-1} at RT	Promising for Na-metal batteries	Quasi-solid/IL-laden system; ionic liquid content and cation transference need careful reporting	[90]
	NaFSI/[EMIM][FSI]@UiO-66	FSI-based Na ionic liquid confined in UiO-66 pores	Na^+	10^{-4}-10^{-3} S·cm^{-1} at RT	FSI chemistry can enhance ion mobility relative to bulkier TFSI systems	FSI-based systems may raise interfacial/corrosion concerns; still liquid-containing	[91]
	Na[EMIM][TFSI]@Zn-MOF-74	Na-containing EMIM/TFSI ionic phase in 1D MOF-74 channels with open metal sites	Na^+	5×10^{-4} S·cm^{-1} at RT	Synergistic ion transport through MOF-74 one-dimensional channels and ionic liquid; Promising for Na-metal batteries	Poor moisture stability and open metal site interactions can trade off conductivity and long-term stability	[59]
	a_gZW-UiO-67·MSA	Zwitterion-grafted UiO-67 plus Brønsted acid; MIMS-MSA acid-base subsystem provides proton transport in melt-quenched glass	H^+	1.57×10^{-2} S·cm^{-1} at 100 °C	Breakthrough in glass formation of carboxylate MOFs	Proton conductor, not Li^+/Na^+/K^+ electrolyte; requires acid/zwitterion modification and elevated temperature	[92]
Carboxylate MOF glass	a_g ZW-UiO-68·MSA and a_gZW-DUT-5·MSA	Zwitterion/acid-enabled glass formation in Zr/Al carboxylate frameworks	H^+/potential platform	Glass formation shown; T_m ~156 °C for ZW-UiO-68·MSA and ~152 °C for ZW-DUT-5·MSA	Low-melting carboxylate MOF glasses	Alkali-ion battery conductivity not yet benchmarked; should be framed as material-platform evidence, not Li/Na/K electrolyte performance	[92]
	Mg/Mn adipate-based carboxylate MOF glasses	Flexible aliphatic carboxylate network; melt-quenched Mg^{2+}/Mn^{2+} adipate glasses	No battery ion reported	T_m ~284 °C (Mg) and ~238 °C (Mn); improved hardness/elastic modulus compared with typical ZIF glasses	Low-melting carboxylate MOF glasses	No Li^+/Na+/K^+ conductivity yet; mainly structural/mechanical evidence	[66]

Cu-based MOF + IL	[DEME][TFSI]@HKUST-1	IL confined in HKUST-1 pores; Cu paddlewheel framework provides polar host environment	Li^+	4.0×10^{-4} S·cm^{-1} at RT	High RT conductivity among IL@MOF systems	HKUST-1 has moisture sensitivity; Cu sites/framework stability should be considered for battery compatibility	[93]
	[EMIM][TFSI]@ HKUST-1	Ionic liquid-based ionogel provides the main ion-conducting phase; LLZO ceramic core contributes Li^+ conduction pathways; MOF shell offers porous channels and metal sites for ion regulation/selectivity	Li^+	3.87×10^{-4} S·cm^{-1} at RT	High ionic conductivity, wide electrochemical window, high thermal stability, improved Li dendrite suppression and stable Li metal cycling	Composite system rather than intrinsic MOF or MOF-glass conductor; Li^+ transference number of ionogel electrolytes remains a key concern; performance depends on IL content, interfacial wetting, and core-shell filler dispersion	[94]
Phosphate-based coordination-polymer glass	$[Zn_3(H_2PO_4)_6(H_2O)_3]$ (1,2,3-benzotriazole) glass	Metal phosphate/azole coordination polymer glass; phosphate groups and azole assist anhydrous proton hopping	H^+	8.0×10^{-3} S·cm^{-1} at 120 °C	Anhydrous proton conduction combined with glass processability	Proton conductor at elevated temperature, not alkali-ion battery electrolyte; moisture/temperature dependence must be distinguished from Li/Na/K systems	[95]

LiTFSI: Lithium bis(trifluoromethanesulfonyl)imide; NaTFSI: sodium bis(trifluoromethanesulfonyl)imide; [EMIM][TFSI]:1-ethyl-3-methylimidazolium bis(trifluoromethanesulfonyl)imide; [BMP][TFSI]:1-butyl-1-methylpyrrolidinium bis(trifluoromethanesulfonyl)imide; [EMIM][FSI]: 1-ethyl-3-methylimidazolium bis(fluorosulfonyl)imide; NaFSI: sodium bis(fluorosulfonyl)imide; MAS: methanesulfonic acid; [DEME][TFSI]: N,N-diethyl-N-methyl-N-(2-methoxyethyl) ammonium bis (trifluoromethanesulfonyl)imide; MOF: metal-organic framework; ZIF: zeolitic imidazolate framework; IL: ionic liquid; QSSE: quasi-solid-state electrolyte; PEO: polyethylene oxide; PGZ: poly(1,3-dioxolane) (PDOL)/glassy ZIF-62; PMG-GPE: porous MOF glass gelled polymer electrolyte; SSE: solid-state electrolyte; RT: room temperature; EMIM: 1-ethyl-3-methylimidazolium; TFSI: bis(trifluoromethanesulfonyl)imide; FSI: bis(fluorosulfonyl)imide; MIMS: 1-(1-methyl-3-imidazolio)propane-3-sulfonate; LLZO: lithium lanthanum zirconium oxide.

thereby lowering the energetic barriers associated with melting and vitrification. These topology-driven strategies highlight that glass formation in MOFs is governed not only by local bond chemistry but also by collective network constraints. In ZIFs, works have shown that partial substitution or mixing of metal nodes (e.g., Zn/Co) enables continuous modulation of metal-ligand bond strength thereby systematically lowering the melting temperature and expanding the glass-forming window[99,100]. There have been studies clearly demonstrating that simply changing the metal center can transform an otherwise non-meltable framework into one exhibiting reversible melting behavior[101]. At the microscopic level, metal-node engineering alters local coordination geometry, electronic structure, and metal-organic bond energetics.

Early work by Bennett *et al.* targeted linker substitution in ZIFs - where a fraction of imidazolate linkers in ZIF-4 ($Zn(Im)_2$) is replaced during synthesis by bulkier benzimidazolate or methylbenzimidazolate ligands to form TIF-4 and ZIF-62 - systematically lowers the melting temperature from ~863 K (ZIF-4) to ~740 K (TIF-4) and ~710 K (ZIF-62), suppresses reconstructive recrystallization, and enables direct melt-quenching into a glass while preserving local Zn-N coordination[31]. Building on this foundation, recent studies by Xue *et al.* demonstrated that even highly stable carboxylate-based frameworks, such as UiO-67 and DUT-5, can be rendered meltable through reductions in network connectivity, or cooperative interactions with pore-confined guests[92]. From a thermodynamic perspective, topology-driven strategies effectively reduce the rigidity of the coordination network, increase structural degrees of freedom, and enhance defect tolerance, thereby lowering the energetic barriers associated with melting or vitrification[12].

A promising strategy: molten salt

Building on the diverse strategies developed for ion-conducting MOF glasses, we further propose that molten-salt chemistry may offer a useful conceptual framework for designing and understanding ion-conducting MOF glasses. This perspective is inspired by molten-salt strategies widely used in carbon and oxide chemistry, where molten salts can act not only as ion reservoirs, but also as reaction media, fluxes, structure-directing agents, and thermal stabilizers. When translated to MOF-glass systems, molten salts may play multiple roles: they can introduce mobile alkali-metal carriers, weaken or screen metal-ligand interactions, lower the effective melting or softening temperature, suppress premature framework decomposition, and facilitate vitrification during quenching. In our view, four coupled mechanisms are particularly relevant when translating these approaches to salt-assisted MOF systems, as demonstrated in Figure 11.

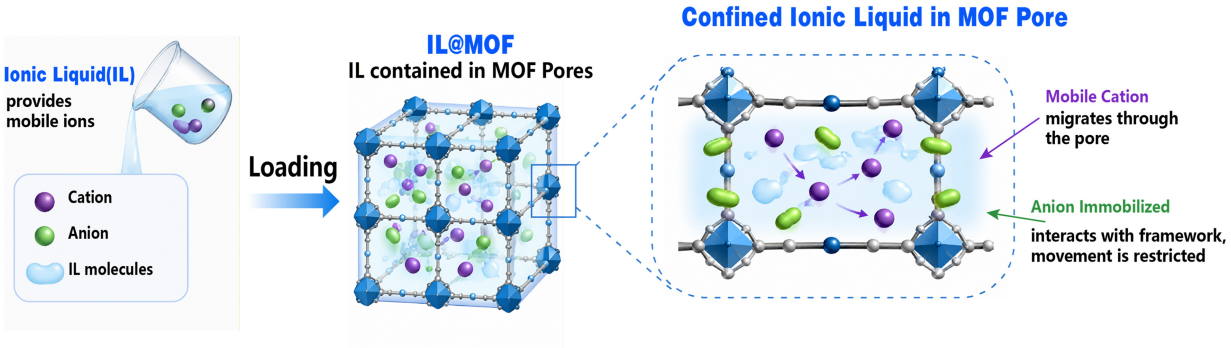

Figure 9. Ion-transport mechanism in IL@MOF electrolytes. Alkali-metal-ion-containing ionic liquids are loaded into MOF nanopores to form IL@MOF hybrid electrolytes. Within the confined MOF channels, Li^+ or Na^+ cations can migrate along the pore network, whereas bulky anions interact with the MOF framework and exhibit restricted mobility. The confinement effect and framework-anion interactions can facilitate cation-dominated ion transport. MOF: Metal-organic framework; IL: ionic liquid.

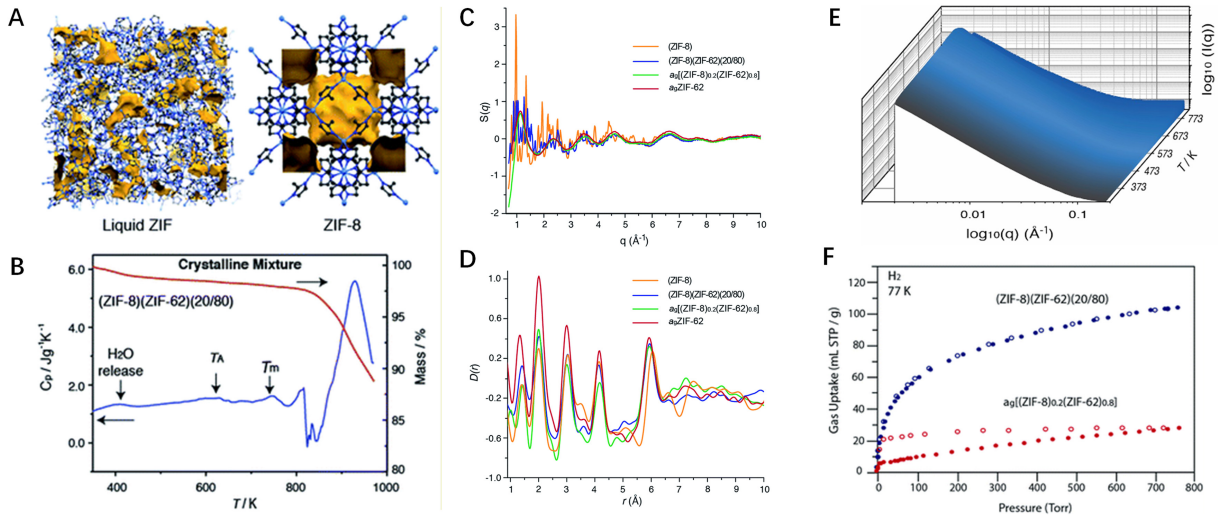

Figure 10. Dissolving ZIF-8 by ZIF-62. (A) Atomic configuration of a high-temperature liquid ZIF; (B) C_p and mass as a function of temperature for (ZIF-8)(ZIF-62) (20/80); (C) Structure factors S(q) of (ZIF-8)(ZIF-62) (20/80), $a_g[(ZIF\text{-}8)_{0.2}(ZIF\text{-}62)_{0.8}]$ and ZIF-8, alongside that of a_gZIF-62; (D) Corresponding X-ray pair distribution functions D(r); (E) Temperature resolved SAXS profile of (ZIF-8)(ZIF-62) (20/80); (F) H_2 at 77 K gas isotherms for the zinc-based crystalline mixtures and glasses. (A-F) adapted with permission from reference[98]. Copyright 2019, Royal Society of Chemistry. SAXS: Small-angle X-ray scattering; ZIF: zeolitic imidazolate framework.

Halide or mixed chloride salts behave as low-viscosity ionic fluxes. They provide a continuous liquid environment that dramatically accelerates mass transport and lowers kinetic barriers for bond exchange and framework rearrangement. When a crystalline MOF is immersed in such a molten-salt medium, the framework no longer needs to reach its intrinsic melting point to undergo large-scale reorganization; instead, depolymerization-repolymerization events can be triggered at significantly reduced temperatures within the salt flux. This is mechanistically analogous to flux-melting using a low-T_m MOF glass, but the role of the liquid phase is now played by an inorganic salt.

Second, molten salts are not inert solvents. Their highly polarizable anions (e.g., Cl^-) and small, strongly coordinating cations can directly interact with metal-ligand bonds in the MOF[102]. At the microscopic level, these ions compete with the original linkers for coordination to the metal nodes and screen metal-ligand electrostatics. This weakens metal-ligand coordination, promotes linker cleavage, and locally depolymerizes the network, effectively softening the framework. In ZIFs, for example, partial replacement of Zn-imidazolate coordination by

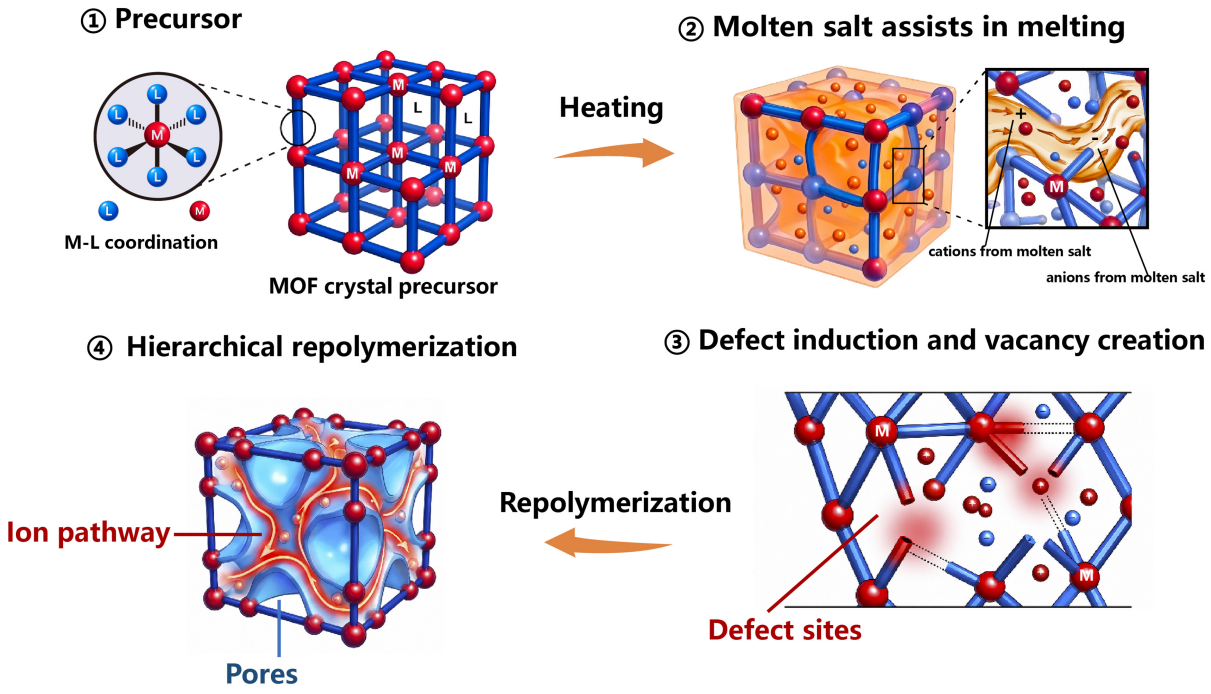

Figure 11. Coupled mechanism for molten-salt-assisted ionic conductive MOF glass.

halide or alkali-ion coordination can facilitate Zn-N bond rearrangement, thereby lowering the thermal transition temperatures and enabling access to a viscous, melt-like state before decomposition[54,68,97].

Besides, the molten-salt environment also exerts a spatial confinement effect. In a salt-filled pore space, the surrounding ionic medium acts as a liquid matrix that limits crystallite growth, suppresses sintering, and stabilizes highly defective or partially depolymerized states that would be unstable in the absence of the salt. Once incorporated into the softened coordination network, ionic species such as Li^+, Na^+, and Cl^- can act as network modifiers and become integrated into the local coordination structure rather than simply occupying residual pore space[54]. Their incorporation creates chemically heterogeneous coordination environments, including undercoordinated alkali-ion sites and mixed metal-linker/halide coordination around the metal nodes[68]. Meanwhile, the dynamic disruption and reformation of metal-linker-metal bridges during vitrification increases the population of non-bridging or dangling linkers and undercoordinated metal sites, resulting in a more depolymerized and structurally heterogeneous glass network[103].

Once vitrification occurs, the same ions that acted as flux now play a second role: they form nanoconfined ionic domains within the amorphous framework. In pores, interstitial regions, and defect-rich zones, the molten salt behaves as a highly dissociated ionic medium. Under nanoconfinement, its structure and dynamics differ from the bulk, but the effective ion mobility can remain high[104,105]. The result is a percolating network of salt-rich pathways threaded through a mechanically robust MOF glass matrix. From the perspective of ionic conductivity, this hybrid state combines (i) the isotropic, macroscopically grain-boundary-free transport of a glass with (ii) continuous, liquid-like ion highways provided by the nanoconfined salt.

CHARACTERIZATION OF MOF-GLASS-BASED SSEs

For accurately determining the ionic conductivity of MOF glasses, it is essential to exclude possible contributions from electronic and protonic conduction. A combination of characterization methods, including Arrhenius/Vogel-Tamman-Fulcher (VTF) fitting, activation energy analysis, and direct current (DC) polarization measurements, can be used to more precisely define their ion-conducting behavior.

Meanwhile, understanding the active sites and functional components within MOF glasses is crucial for the rational design and optimization of MOF glass-based SSEs. Short-range or local probes, such as X-ray photoelectron spectroscopy (XPS) and electron microscopy, can provide information on the chemical states of elements in MOFs. However, these techniques are limited in their ability to deliver atomically resolved insights, such as the precise coordination environments, electronic characteristics of incorporated species, and the nature of active sites. In this context, the growing need for advanced characterization and analytical techniques has great significance to the field of MOF glass ionic conductors.

Conductivity characterization

Temperature-dependent electrochemical impedance spectroscopy and conductivity fitting

Temperature-dependent electrochemical impedance spectroscopy (EIS) has been widely used to evaluate ionic conductivity and transport mechanisms in MOF-based and MOF-glass-based electrolytes[106]. In these systems, impedance spectra are collected at different temperatures to extract the electrolyte resistance, and the conductivity is calculated based on the sample geometry. However, recent studies have emphasized that EIS-derived conductivity values in MOF electrolytes should be interpreted cautiously, because residual solvent, adsorbed water, proton conduction, electrode polarization and interfacial artefacts can all contribute to the measured impedance response[13]. Therefore, temperature-dependent EIS is often combined with conductivity fitting to provide mechanistic insight rather than only a single conductivity value[13].

Arrhenius fitting is commonly used when ion transport follows a thermally activated hopping mechanism. By plotting conductivity as a function of inverse temperature, the apparent activation energy can be extracted from the slope. Previous studies on MOF-glass-based electrolytes have commonly employed temperature-dependent conductivity measurements and Arrhenius analysis to evaluate ion-transport behavior, where the activation energy provides a useful descriptor for assessing how glass formation, structural disorder, and ion-conducting pathways influence ion migration[107,108].

Nevertheless, ion transport in disordered glassy systems may not always follow simple Arrhenius behavior[109]. In conventional glass ionics, non-Arrhenius conductivity has been attributed to factors such as a distribution of activation energies arising from structural disorder[110]. This suggests that the apparent activation energy may vary with temperature, particularly when the conducting matrix undergoes structural relaxation or dynamic rearrangement. For MOF glass, when near or above T_g, viscosity evolution becomes strongly coupled to framework dynamics, where increasing thermal energy promotes local coordination fluctuations and enhanced segmental mobility within the disordered network. As described by VTF behavior, ion conductivity in many MOF glasses deviates from simple Arrhenius transport above T_g due to the viscoelastic nature of the glassy matrix[26]. This suggests that ion transport near T_g is not solely governed by static hopping pathways, but is intrinsically linked to thermally activated framework relaxation and dynamic disorder within the coordination network. In these cases, VTF analysis may provide a more appropriate description of non-Arrhenius conductivity behavior, especially for MOF-glass-based electrolytes where ion migration is strongly coupled to matrix mobility. Therefore, comparing Arrhenius and VTF fitting can help distinguish between relatively static hopping-dominated transport and dynamically coupled ion transport associated with glassy-network relaxation.

Therefore, EIS, Arrhenius fitting and VTF fitting can be considered as an integrated characterization module for MOF-glass ionic conductors. EIS provides the conductivity values, Arrhenius fitting reveals the apparent activation energy for thermally activated hopping, and VTF fitting helps identify whether ion transport is coupled with the dynamic relaxation of the amorphous or polymeric matrix. This combined analysis is essential for understanding how glass formation, guest incorporation and MOF-glass interactions influence ionic conduction in MOF--glass-based solid electrolytes[81].

DC polarization

Electrochemical impedance spectroscopy is commonly used to determine the total ionic conductivity of MOF-glass-based electrolytes by extracting the bulk or total resistance from the impedance spectra[25,39]. However, EIS alone cannot fully distin-

guish ionic conduction from possible electronic contributions. Therefore, direct current polarization measurements are often employed as a complementary method to evaluate the electronic conductivity and ionic transference number. Under a constant direct current bias with ion-blocking electrodes, mobile ions accumulate at the electrode-electrolyte interfaces, causing the current to decay with time, whereas the remaining steady-state current is mainly associated with electronic conduction. A negligible steady-state current therefore indicates that the measured conductivity is dominated by ion transport rather than electronic leakage[111-113].

DC polarization measurements are necessary for MOF-glass electrolytes because the measured conductivity may be affected by various non-target charge-transport processes. Metal nodes, coordinatively unsaturated sites, and structural defects in MOF glasses may form local electronic transport pathways, thereby introducing a certain degree of electronic conductivity. Incompletely removed guest molecules, moisture, or residual salts may also participate in protonic, ionic, or electronic transport, making it more difficult to determine the true origin of the measured conductivity[114]. For MOF glasses prepared through high-temperature treatment, partial carbonization, thermal decomposition, or structural rearrangement may further generate electronically conductive components. This issue becomes particularly important for halide- or metal-salt-modified MOF glasses, such as those incorporating LiCl, NaCl, or AgI, where increased conductivity does not necessarily originate solely from enhanced migration of the target ions, but may also include contributions from electronic leakage, interfacial polarization, or side reactions[27]. Therefore, DC polarization measurements are essential for excluding electronic conduction and confirming ion-dominated transport behavior in MOF-glass electrolytes[81].

Structure characterization

X-ray absorption spectroscopy: detecting atomic structure

X-ray absorption spectroscopy (XAS) is an effective technique for investigating the local electronic structure of atoms and their coordination environments within MOF glass structures[31]. X-ray absorption near-edge structure (XANES) can reveal the oxidation state and local electronic structure of atoms, while EXAFS can probe the bond distances to neighboring atoms and their coordination numbers[115,116]. Xue *et al.* used Zr K-edge XANES and EXAFS to analyze the local structure of a family of carboxylate MOFs[92]. XAS provides element-specific insight into the local structure of MOF glasses. The Zr K-edge XANES spectra of ZW-UiO-67·MSA before and after vitrification show only minor changes, indicating that the local electronic state and coordination environment of Zr are largely preserved during glass formation [Figure 12A]. A similar result is observed for ZW-UiO-67·TFSA, further supporting the retention of the local Zr environment after vitrification [Figure 12B]. The corresponding Fourier-transformed extended X-ray absorption fine structure (FT-EXAFS) spectra of ZW-UiO-67·MSA exhibit closely related first- and higher-shell features before and after vitrification, suggesting that the local Zr-O coordination shell and Zr-based node structure remain substantially intact in the glassy phase [Figure 12C]. Likewise, the FT-EXAFS spectra of ZW-UiO-67·TFSA confirm that the local coordination motifs are largely maintained despite the loss of crystallographic long-range order [Figure 12D]. Together, these results show that MOF vitrification primarily disrupts long-range periodicity while preserving the essential local coordination framework.

PDF: quantitative insight into the structural coherence of materials by total scattering

Although XRD is commonly used to investigate the long-range ordered structures of MOFs, X-ray total scattering combined with PDF analysis focuses on short- and medium-range structural order, thereby complementing XAS[117,118]. X-ray diffuse scattering patterns collected at high scattering-vector regions can be transformed through inverse Fourier transformation to extract short- and medium-range structural information, as they provide the probability of finding pairs of atoms separated by a distance r[119,120]. Therefore, PDF analysis is particularly useful for elucidating the mechanisms associated with linker functionalization, defect formation in MOFs, and the formation or transformation of metal nodes[121]. Meanwhile, the PDF can be calculated from a known MOF glass structure and can provide a local view of the material's structure. This mathematical representation therefore offers a local perspective on the structural arrangement, as if an observer were

standing on an atom and examining its surrounding environment.

THz/far-IR: probing metal bond and inorganic

Terahertz/far-infrared (THz/far-IR) spectroscopy is an effective technique for probing the quasi-localized properties and bonding characteristics of MOF composites. Through *in situ* THz/far-IR measurements, further information on the evolution of these composites during MOF formation can be collected. As Figure 13A shows, our team has applied this technique for the first time to reveal the dynamic behavior of glassy MOF-perovskite composites during the sintering process[122].

In another study [Figure 13B], our team employed this technique to monitor the metal-N bonding environment in modified ZIF-62(Co)[123]. In a_gZIF-62(Co)-Fe, the broad Co-N band at approximately 334 cm^{-1} is consistent with structural amorphization, while the newly emerged peak at around 344 cm^{-1} indicates the formation of Fe-N stretching vibrations[123].

PALS: revealing free-volume defects and nanoscale voids

PALS has emerged as a particularly informative probe for characterizing nanoscale free volume, inaccessible microporosity, and defect-related cavities in MOF glasses. PALS can measure the lifetime of positronium species localized within low-electron-density regions, allowing characteristic cavity sizes and pore-size distributions to be inferred from positronium annihilation behavior. This capability has been demonstrated across several MOF-glass systems, including ZIF-62 glasses with exceptional glass-forming ability, ZIF-62-derived glass membranes, and ZIF-76-based glasses with permanent accessible porosity[37,40,49,124]. These studies collectively establish PALS as a valuable complementary technique for evaluating how vitrification reshapes the intrinsic free volume and porosity of MOF-derived glassy networks.

A representative example is provided by Thornton *et al.* in their study of porosity in MOF glasses[46]. In this work, PALS was used to compare the pore-size distributions of crystalline ZIF-4, dense crystalline ZIF-zni, and melt-quenched a_gZIF-4. As shown in Figure 14, the PALS-derived pore-size distributions reveal that a_gZIF-4 possesses a pore structure intermediate between the open framework ZIF-4 and the denser ZIF-zni phase, while also exhibiting a broader distribution characteristic of a structurally disordered glassy network[46]. This example illustrates the specific value of PALS for identifying nanoscale vacancies, voids, and defect-like free-volume elements that may persist after framework collapse or vitrification, including pore environments that may be inaccessible to gas adsorption measurements.

For ion-conducting MOF glasses, such information is particularly significant. Ionic transport in disordered hybrid glasses may be influenced not only by the chemical coordination environment of mobile ions, but also by the size, distribution, and possible connectivity of free-volume elements or defect-rich regions within the glassy framework. PALS therefore has strong potential to serve as a structural probe for assessing whether enhanced ionic conductivity correlates with increased free volume, nanoscale void formation, or defect-mediated transport pathways. However, this interpretation should be made cautiously: PALS does not directly measure ion mobility or prove an ion-conduction mechanism. Rather, it provides critical structural evidence that should be correlated with electrochemical impedance spectroscopy, ion transference measurements, solid-state NMR, XPS/XAS, and local-structure analyses to establish a more complete relationship between free volume, defect structure, and ion transport in MOF glass electrolytes.

CONCLUSION AND OUTLOOK

Future applications

The structural programmability of MOF glasses provides a promising platform for developing next-generation solid-state ion conductors. MOF glasses exhibit features including disorder in long-range yet remain chemically tunable coordination networks, sub-nanometer free volume, dynamic metal-ligand environments, and macroscopically grain-boundary-free monolithic architectures, which create opportunities to design ion-transport pathways that are not limited to intrinsic crystallographic pores, but can instead be regulated through glass composition, coordination chemistry, defect concentration, free-volume distribution, and thermal history.

One particularly attractive direction is the develop-

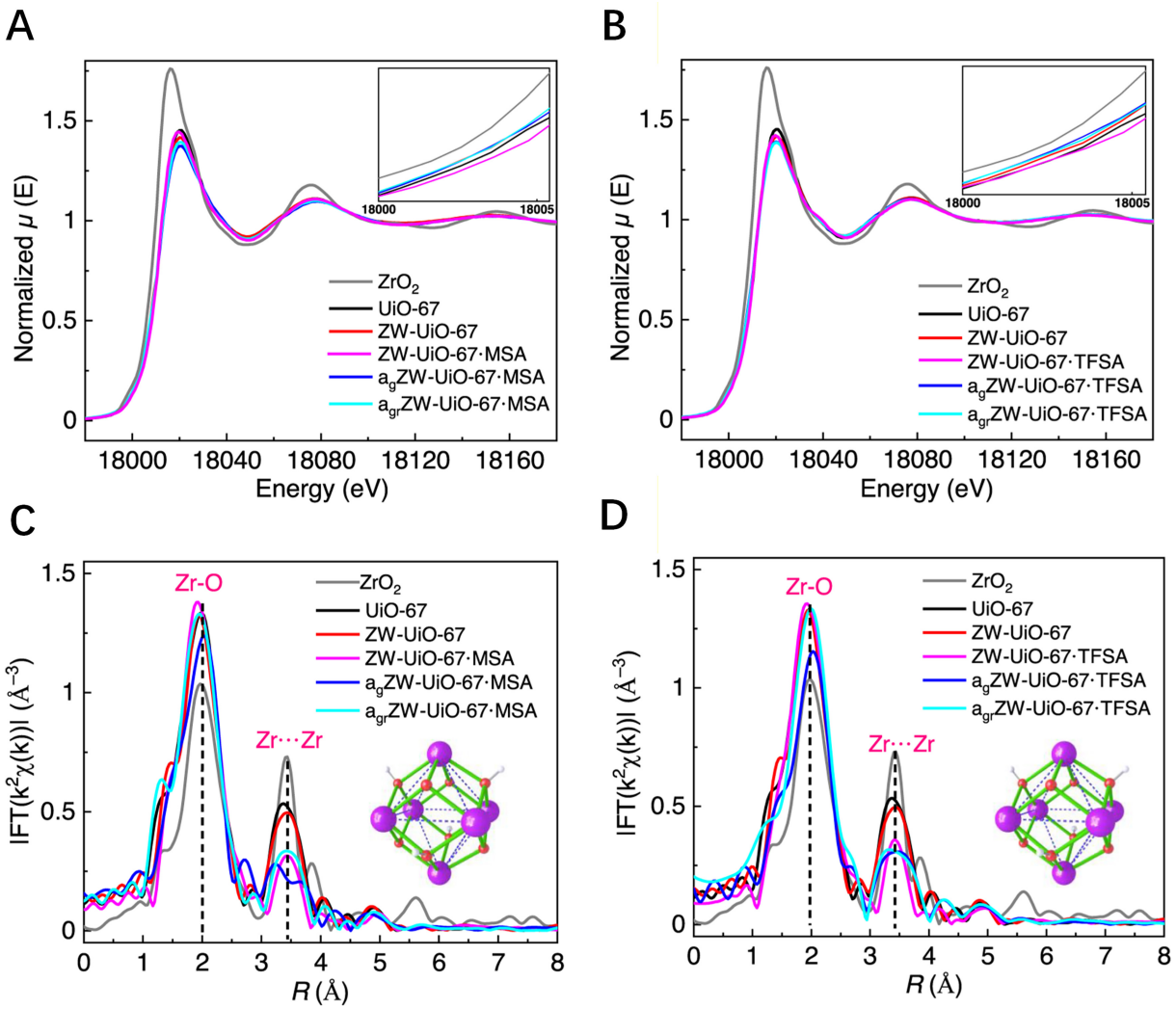

Figure 12. Zr K-edge X-ray absorption spectroscopy analysis of ZW-UiO-67-based glasses. (A) XANES spectra at the K-edge of the Zr atoms for derivatives of ZW-UiO-67·MSA and references; (C) Corresponding radial distance χ(R) space spectra from k^3-weighted Fourier transform of χ(k)-function from the Zr K-edge EXAFS. Comparison spectra for ZW-UiO-67·TFSA and derivatives are shown in (B) and (D). Insets in (C) and (D) show the octahedral $Zr_6O_4(OH)_4$ node. Color codes: Zr, purple; O, red; H, light gray. (A-D) Reproduced from reference[92], licensed under CC BY 4.0. MOF: Metal-organic framework; XANES: X-ray absorption near-edge structure.

ment of salt-assisted MOF-glass electrolytes. The incorporation of light-metal halide salts, such as LiCl or NaCl, may serve a dual function: reducing the effective vitrification barrier of rigid coordination frameworks and simultaneously introducing mobile ionic carriers. This approach may expand MOF-derived glasses beyond intrinsically meltable ZIF systems to include frameworks that are traditionally difficult to vitrify. If the salt-framework interaction is properly controlled, such modified glasses have the potential to exhibit even higher ion conductivity than pristine MOF glass under near-room-temperature or moderately elevated-temperature conditions, thereby occupying an important materials space between polymer electrolytes and ceramic solid electrolytes.

Hybrid MOF glasses are also promising for ion conduction and may be deployed in intermediate-temperature solid-state batteries, particularly sodium- and lithium-based stationary energy-storage systems. Their amorphous and isotropic nature can suppress grain-boundary resistance, improve interfacial conformity with electrodes, and provide mechanically adaptable electrolyte layers. At temperatures approximating the glass transition point, partial softening of the coordination network may enhance local structural dynamics, promote ion mobility, and improve electrode reaction kinetics, while avoiding the severe thermal-management

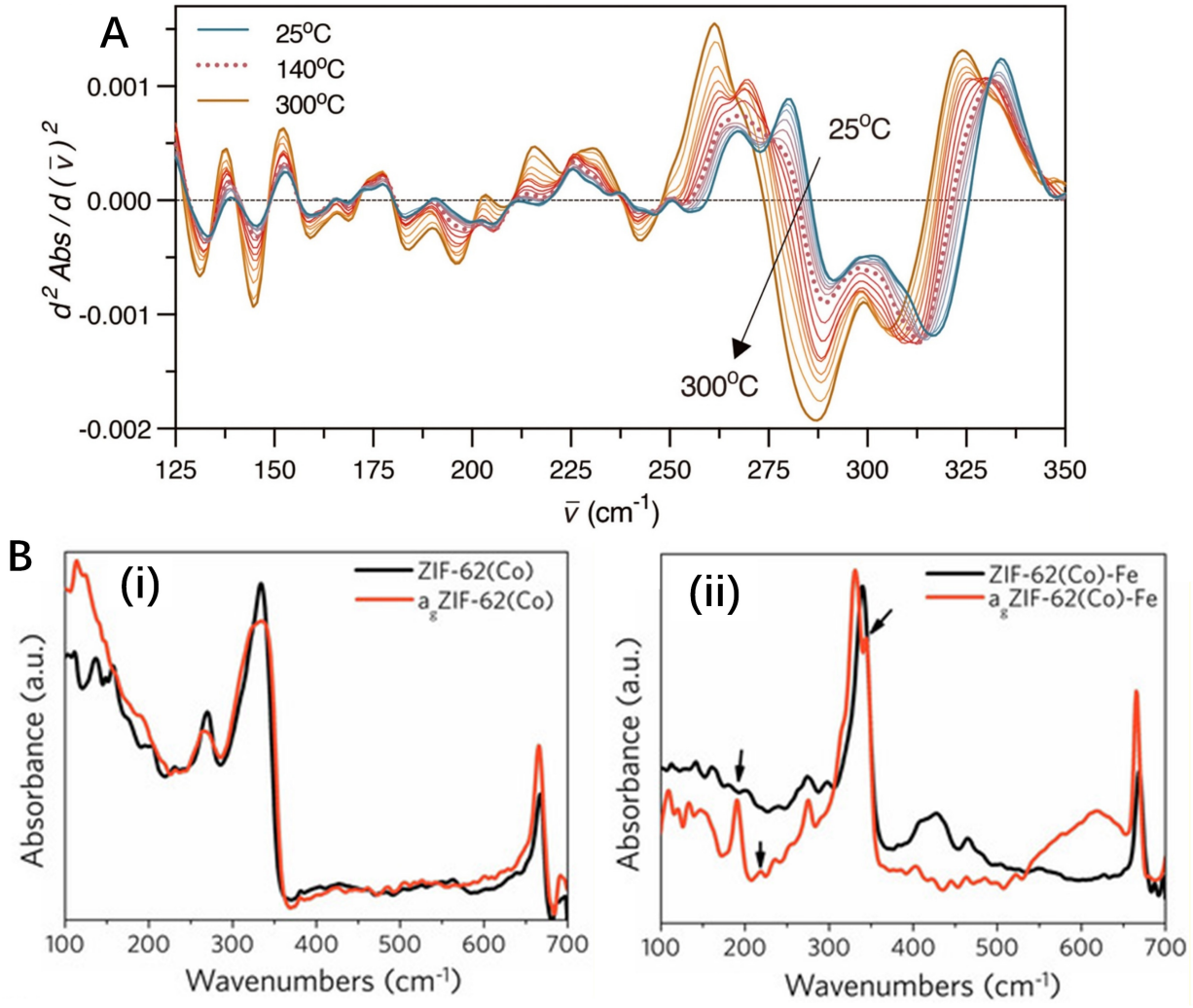

Figure 13. (A) *In situ* THz/far-IR spectroscopy for monitoring temperature-dependent bonding evolution during sintering; (B) ZIF-62(Co)Fe before and after sintering. (i) Larger Co-N peak after vitrification; (ii) Fe-N formation after heating. (A) adapted with permission from reference[122]. Copyright 2021, American Association for the Advancement of Science; (B) is adapted with permission from reference[123]. Copyright 2022, Wiley-VCH GmbH.

requirements associated with conventional high--temperature ceramic electrolytes. These advantages are especially relevant for stationary batteries, where long-term durability, processability, and interfacial stability are often more important than maximum gravimetric energy density.

Moreover, as demonstrated by Ogawa *et al.*, beyond alkali-metal-ion conduction, MOF glasses offer considerable potential as anhydrous or low-humidity proton conductors[39]. The combination of coordinatively unsaturated metal sites, hydrogen-bonding ligands, phosphate- or sulfonate-containing units, and nanoconfined ionic domains could generate proton-transfer pathways that remain active under conditions where hydrated polymer membranes lose performance. This makes MOF-glass electrolytes attractive for intermediate-temperature proton-conducting fuel cells, membrane reactors, and electrochemical hydrogen-separation devices. Compared with conventional polymer membranes, MOF glasses may provide improved thermal robustness, reduced dehydration sensitivity, and more chemically programmable proton-transfer environments.

Another important application area is ion-selective membranes and electrochemical separation devices. Wang *et al.* have initiated investigations into MOF glass composites for lithium enrichment[125]. Because the ionic species, coordination sites, and free-volume architecture can be independently tuned, MOF glasses could be engineered for selective transport of

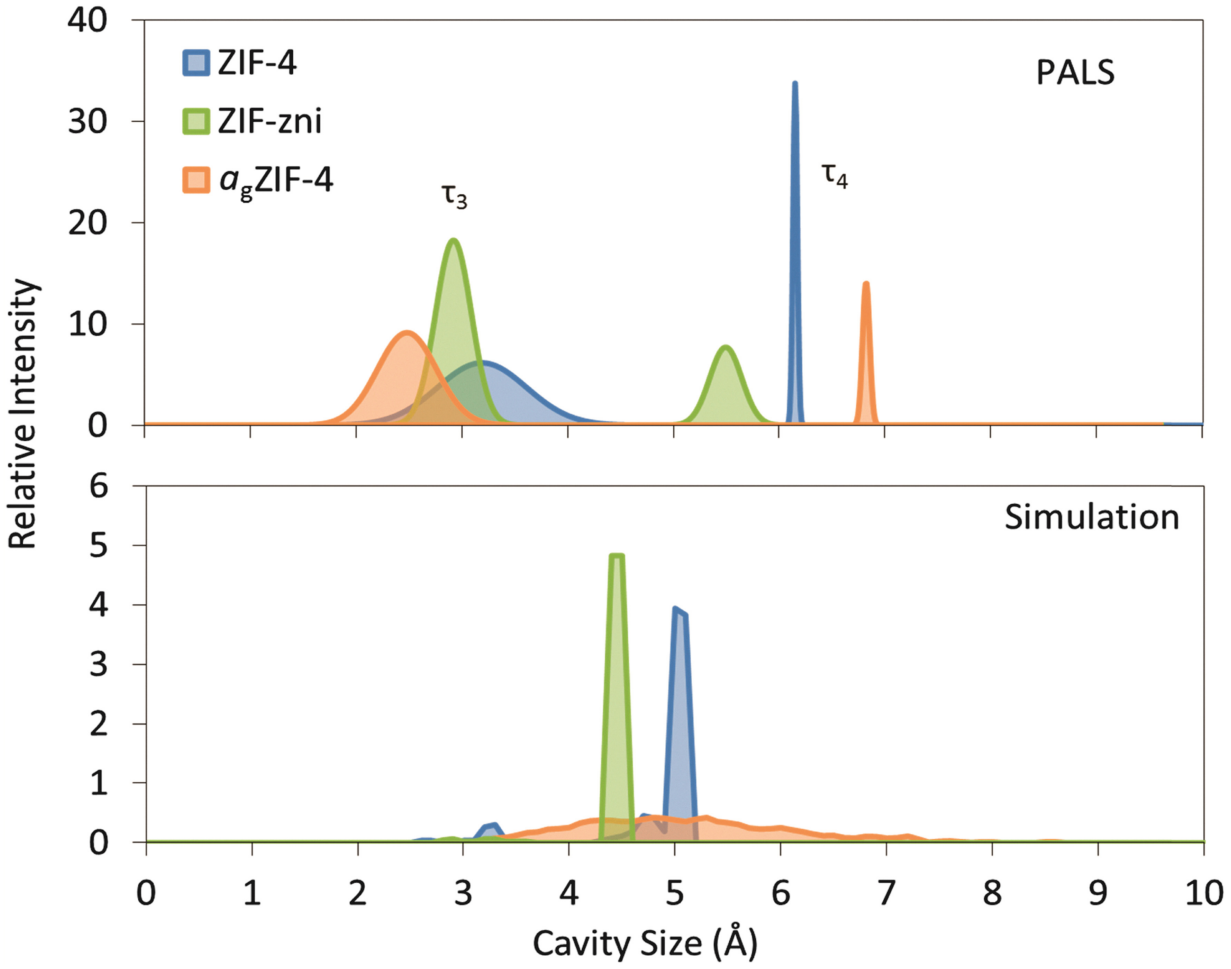

Figure 14. Pore size distributions measured with PALS and simulated with *Zeo++* for ZIF-4, ZIF-zni and a_gZIF-4. PALS results for the third and fourth components (τ3 and τ4) are represented as Gaussian distributions which correspond to the small and large cavities, respectively. This figure is quoted with permission from reference[46], licensed under CC BY 3.0. PALS: Positron annihilation lifetime spectroscopy.

Li^+, Na^+, K^+, Ag^+, H^+, or multivalent ions. The absence of grain boundaries may also reduce non-selective leakage pathways, which is a major limitation in many polycrystalline ion-conducting membranes.

MOF-glass ion conductors may further contribute to solid-state sensors and harsh-environment ionic devices. Their compositional flexibility, thermal stability, and resistance to grain-boundary degradation make them suitable for gas sensors, humidity sensors, electrochemical probes, and high-temperature ionic devices. By selecting appropriate metal nodes, ligands, and incorporated salts, the transport response could be coupled with specific chemical stimuli, enabling ion-conducting glasses with sensing functions.

More broadly, the key opportunity lies in transforming meltability from a rare intrinsic property into a programmable design parameter. Through flux-assisted vitrification, coordination-environment modulation, and compositing or interface-mediated transport design, MOF glasses could evolve from a small family of meltable ZIF-derived materials into a broader class of processable ionic glasses.

Challenges

Despite these opportunities, several fundamental and technological challenges must be addressed. The first challenge is to establish reliable structure-transport relationships. Ion conduction in MOF glasses is expected to involve multiple coupled factors, including free-volume size, defect concentration, metal-ligand bond dynamics, salt distribution, local coordination disorder, and segmental motion near the glass transition temperature. However, these factors

are difficult to decouple experimentally. A high apparent conductivity alone is insufficient to prove efficient ionic transport; it must be supported by activation-energy analysis, isotope-effect measurements, DC polarization, impedance spectroscopy using appropriate blocking and non-blocking electrodes, and structural probes such as PDF, EXAFS, PALS, and variable-temperature spectroscopy as discussed in Section "CHARACTERIZATION OF MOF--GLASS-BASED SSEs".

Long-term stability is another central concern. Salt-assisted vitrification and ion incorporation may create metastable structures that are beneficial for transport but vulnerable to structural relaxation, salt redistribution, phase segregation, or crystallization during extended operation. Repeated thermal cycling, operation near or above T_g, electrochemical bias, and contact with reactive electrodes may progressively alter the defect population, free-volume distribution, and local coordination environment. Understanding how ionic mobility couples with glass relaxation will therefore be essential for predicting lifetime performance.

Device integration also remains nontrivial. Although the amorphous and isotropic nature of MOF glasses may improve physical contact with electrodes compared with rigid crystalline ceramics, the formation of interphases at electrode-electrolyte boundaries remains poorly understood. Interfacial resistance, electrode compatibility, redox stability, dendrite suppression in metal batteries, and mechanical integrity under cycling must be systematically evaluated. The electrochemical stability window of each MOF-glass electrolyte should also be carefully determined, since organic ligands, redox-active metal nodes, and incorporated salts may introduce decomposition pathways under bias.

Scalable synthesis and processing are also key barriers. Electrolytes typically require homogeneous composition and compatibility with established workflows. Achieving these requirements for fabricating MOF glass ion conductor at large scale is challenging because small variations in precursor crystallinity, particle size, salt loading, heating rate, pressure, or quenching conditions may strongly influence glass structure and ionic conductivity. Future work should therefore move beyond small bulk pellets toward thin films, supported membranes, laminated electrolytes, and prototype cells.

For solid-state battery applications, the practical viability of MOF glass electrolytes should be evaluated beyond ionic conductivity. Key issues include the electrochemical stability window, chemical compatibility with metal anodes, oxidative stability against high-voltage cathodes, interfacial decomposition, and dendrite suppression. Previous studies have shown that many solid electrolytes are not thermodynamically stable against alkali-metal electrodes and may form resistive decomposition interphases during cycling[126,127]. Moreover, interfacial instability can increase cell resistance, promote uneven metal deposition, and accelerate dendrite growth[128]. Therefore, future MOF glass electrolytes should be designed with stable electrode interfaces, sufficient mechanical robustness, and suppressed parasitic reactions.

Finally, the field requires clearer performance benchmarks and standardized testing protocols. Conductivity values should be reported together with activation energy, temperature and humidity conditions, sample geometry, electrode configuration, electronic transference number, cycling stability, and post-mortem structural analysis. For battery-related applications, symmetric-cell cycling, full-cell testing, critical current density, and interfacial impedance evolution should be included.

Conclusion

Overall, salt-assisted and structurally modulated MOF glasses offer a promising route to modulate glass formation, coordination chemistry, and ion transport within a single design framework. Their greatest promise lies not simply in achieving ion conductivity, but in enabling processable, chemically programmable, and interface-adaptable ion conductors. If the challenges of mechanistic verification, long-term stability, interfacial compatibility, and scalable processing can be addressed, MOF-glass ion conductors could become a versatile platform for solid-state batteries, proton-conducting devices, ion-selective membranes, and even integrated electrochemical energy systems.

DECLARATIONS

Authors' contributions

Writing and conceptualization: Qu, H.; Huang, W.

Review & editing: Huang, W.; Hou, J.
Project administration: Hou, J.
Funding acquisition: Hou, J.

Availability of data and materials

Not applicable.

AI and AI-assisted tools statement

Not applicable.

Financial support and sponsorship

This work was financially supported by the Australian Research Council (DP230101901, LP220100309, FT210100589). This research was conducted by the ARC Centre of Excellence for Green Electrochemical Transformation of Carbon Dioxide (CE230100017) and funded by the Australian Government.

Conflicts of interest

Hou, J. is an Associate Editor of *Greenverse Science* but was not involved in any aspect of the editorial process for this manuscript, including reviewer selection, manuscript handling, or editorial decision-making. The other authors declared that they have no conflicts of interest.

Ethical approval and consent to participate

Not applicable.

Consent for publication

Not applicable.

Copyright

REFERENCES

1. Casas-Cabanas, M.; Palacín, M. R. Challenges ahead in the development of solid-state batteries. *J. Power. Sources.* **2025**, *659*, 238355. DOI
2. Koech, A. K.; Mwandila, G.; Mulolani, F.; Mwaanga, P. Lithium-ion battery fundamentals and exploration of cathode materials: a review. *S. Afr. J. Chem. Eng.* **2024**, *50*, 321-39. DOI
3. Zhang, Z.; Wang, X.; Li, X.; et al. Review on composite solid electrolytes for solid-state lithium-ion batteries. *Mater. Today. Sustainability.* **2023**, *21*, 100316. DOI
4. Balaish, M.; Gonzalez-Rosillo, J. C.; Kim, K. J.; Zhu, Y.; Hood, Z. D.; Rupp, J. L. M. Processing thin but robust electrolytes for solid-state batteries. *Nat. Energy.* **2021**, *6*, 227-39. DOI
5. Hayashi, A.; Sakuda, A.; Tatsumisago, M. Development of sulfide solid electrolytes and interface formation processes for bulk-type all-solid-state Li and Na batteries. *Front. Energy. Res.* **2016**, *4*. DOI
6. Furukawa, H.; Cordova, K. E.; O'keeffe, M.; Yaghi, O. M. The chemistry and applications of metal-organic frameworks. *Science* **2013**, *341*, 1230444. DOI
7. Horike, S.; Umeyama, D.; Kitagawa, S. Ion conductivity and transport by porous coordination polymers and metal-organic frameworks. *Acc. Chem. Res.* **2013**, *46*, 2376-84. DOI PubMed
8. Kharod, R. A.; Andrews, J. L.; Dincă, M. Teaching metal-organic frameworks to conduct: ion and electron transport in metal-organic frameworks. *Annu. Rev. Mater. Res.* **2022**, *52*, 103-28. DOI
9. Phang, W. J.; Jo, H.; Lee, W. R.; et al. Superprotonic conductivity of a UiO-66 framework functionalized with sulfonic acid groups by facile postsynthetic oxidation. *Angew. Chem. Int. Ed. Engl.* **2015**, *54*, 5142-6. DOI PubMed
10. Dong, P.; Zhang, X.; Hiscox, W.; et al. Toward high-performance metal-organic-framework-based quasi-solid-state electrolytes: tunable structures and electrochemical properties. *Adv. Mater.* **2023**, *35*, e2211841. DOI PubMed
11. Shen, L.; Wu, H. B.; Liu, F.; et al. Creating lithium-ion electrolytes with biomimetic ionic channels in metal-organic frameworks. *Adv. Mater.* **2018**, *30*, e1707476. DOI PubMed
12. Pallach, R.; Keupp, J.; Terlinden, K.; et al. Frustrated flexibility in metal-organic frameworks. *Nat. Commun.* **2021**, *12*, 4097. DOI PubMed PMC
13. Deriche, Z.; Biswal, S. L.; Kampouri, S. Navigating ionic conductivity in MOF electrolytes: addressing measurement pitfalls and performance limits. *J. Mater. Chem. A.* **2025**, *13*, 33012-33. DOI
14. Zhang, J. P.; Zhou, H. L.; Zhou, D. D.; Liao, P. Q.; Chen, X. M. Controlling flexibility of metal-organic frameworks. *Natl. Sci. Rev.* **2018**, *5*, 907-19. DOI
15. Ji, Z.; Wang, H.; Canossa, S.; Wuttke, S.; Yaghi, O. M. Pore chemistry of metal-organic frameworks. *Adv. Funct. Mater.* **2020**, *30*, 2000238. DOI
16. Taylor, J. M.; Dekura, S.; Ikeda, R.; Kitagawa, H. Defect control to enhance proton conductivity in a metal-organic framework. *Chem. Mater.* **2015**, *27*, 2286-9. DOI
17. Basu, O.; Mukhopadhyay, S.; Laha, S.; Das, S. K. Defect engineering in a metal-organic framework system to achieve super-protonic conductivity. *Chem. Mater.* **2022**, *34*, 6734-43. DOI
18. Chen, Z.; Du, T.; Krishnan, N. M. A.; Yue, Y.; Smedskjaer, M. M. Disorder-induced enhancement of lithium-ion transport in solid-state electrolytes. *Nat. Commun.* **2025**, *16*, 1057. DOI
19. Li, X.; Jiang, G.; Jian, M.; et al. Construction of angstrom-scale ion channels with versatile pore configurations and sizes by metal-organic frameworks. *Nat. Commun.* **2023**, *14*, 286. DOI PubMed PMC

20. Truong, E.; Patel, S. V.; Liu, H.; et al. Accelerating ion transport in polycrystalline conductors: on pores and grain boundaries. *Sci. Adv.* **2025**, *11*, eadt7795. DOI PubMed PMC
21. Shi, Y.; Kimura, S.; Iwai, Y.; et al. Experimental and theoretical investigation of anisotropic proton conduction in two-dimensional metal-organic frameworks. *Inorg. Chem.* **2024**, *63*, 22194-202. DOI PubMed
22. Ding, J.; Du, T.; Jensen, L. R.; et al. High-performance dendrite-free lithium metal anode based on metal-organic framework glass. *Adv. Mater.* **2024**, *36*, e2400652. DOI PubMed
23. Luo, Y.; Li, X.; Liu, L.; Ke, X.; Xu, Y.; Shi, Z. Modification of separator by glassy metal-organic framework with isotropic and grain-boundary-free characteristics enables reversible lithium plating/stripping in lithium metal batteries. *J. Alloys. Compd.* **2026**, *1056*, 186540. DOI
24. Sørensen, S. S.; Østergaard, M. B.; Stepniewska, M.; Johra, H.; Yue, Y.; Smedskjaer, M. M. Metal-organic framework glasses possess higher thermal conductivity than their crystalline counterparts. *ACS. Appl. Mater. Interfaces.* **2020**, *12*, 18893-903. DOI PubMed
25. Wang, X. X.; Guan, D. H.; Miao, C. L.; et al. Boundary-free metal-organic framework glasses enable highly stable all-solid-state lithium-oxygen battery. *Adv. Energy. Mater.* **2023**, *14*, 2303829. DOI
26. Chai, M.; Chen, R.; Xu, K.; et al. Ion transport and conduction in metal-organic framework glasses. *J. Mater. Chem. A.* **2023**, *11*, 20302-14. DOI
27. Jiang, G.; Qu, C.; Xu, F.; et al. Glassy metal-organic-framework-based quasi-solid-state electrolyte for high-performance lithium-metal batteries. *Adv. Funct. Mater.* **2021**, *31*, 2104300. DOI
28. Chen, T.; Reddy, N. P.; Li, M. Enhancing solid-state Li-ion batteries with MOF-polymer composite electrolytes - effect mechanisms and interface engineering. *Gels* **2025**, *11*, 946. DOI
29. Zhao, Y.; Wang, L.; Zhou, Y.; et al. Solid polymer electrolytes with high conductivity and transference number of Li ions for Li-based rechargeable batteries. *Adv. Sci.* **2021**, *8*, 2003675. DOI PubMed PMC
30. Jiang, P.; Du, G.; Cao, J.; et al. Solid-state Li ion batteries with oxide solid electrolytes: progress and perspective. *Energy. Tech.* **2023**, *11*, 2201288. DOI
31. Bennett, T. D.; Yue, Y.; Li, P.; et al. Melt-quenched glasses of metal-organic frameworks. *J. Am. Chem. Soc.* **2016**, *138*, 3484-92. DOI PubMed
32. Umeyama, D.; Horike, S.; Inukai, M.; Itakura, T.; Kitagawa, S. Reversible solid-to-liquid phase transition of coordination polymer crystals. *J. Am. Chem. Soc.* **2015**, *137*, 864-70. DOI PubMed
33. Méndez, E.; Semino, R. Microscopic mechanism of thermal amorphization of ZIF-4 and melting of ZIF-zni revealed *via* molecular dynamics and machine learning techniques. *J. Mater. Chem. A.* **2024**, *12*, 4572-82. DOI
34. Ma, N.; Horike, S. Metal-organic network-forming glasses. *Chem. Rev.* **2022**, *122*, 4163-203. DOI PubMed
35. Bennett, T. D.; Tan, J. C.; Yue, Y.; et al. Hybrid glasses from strong and fragile metal-organic framework liquids. *Nat. Commun.* **2015**, *6*, 8079. DOI PubMed PMC
36. Gaillac, R.; Pullumbi, P.; Coudert, F. X. Melting of zeolitic imidazolate frameworks with different topologies: insight from first-principles molecular dynamics. *J. Phys. Chem. C.* **2018**, *122*, 6730-6. DOI
37. Qiao, A.; Bennett, T. D.; Tao, H.; et al. A metal-organic framework with ultrahigh glass-forming ability. *Sci. Adv.* **2018**, *4*, eaao6827. DOI PubMed PMC
38. Zhou, H. G.; Xia, R. Q.; Zheng, J.; Yuan, D.; Ning, G. H.; Li, D. Acid-triggered interlayer sliding of two-dimensional copper(i)-organic frameworks: more metal sites for catalysis. *Chem. Sci.* **2021**, *12*, 6280-6. DOI PubMed PMC
39. Ogawa, T.; Takahashi, K.; Nagarkar, S. S.; et al. Coordination polymer glass from a protic ionic liquid: proton conductivity and mechanical properties as an electrolyte. *Chem. Sci.* **2020**, *11*, 5175-81. DOI PubMed PMC
40. Jin, X.; Wu, X.; Ng, D.; et al. Liquid metal interface enables glassy MOF membranes with defect-mediated CO_2 transport. *Nat. Commun.* **2025**, *16*, 9510. DOI PubMed PMC
41. Smirnova, O.; Duval, A.; Komal, A.; et al. Unlocking large-area free-standing MOF-glasses for molecular sieving gas separation membranes. *Nat. Commun.* **2026**, *17*, 2575. DOI PubMed PMC
42. Du, T.; Li, S.; Ganisetti, S.; Bauchy, M.; Yue, Y.; Smedskjaer, M. M. Deciphering the controlling factors for phase transitions in zeolitic imidazolate frameworks. *Natl. Sci. Rev.* **2024**, *11*, nwae023. DOI PubMed PMC
43. Kelly, T.; Ghadi, B. M.; Berg, S.; Ardebili, H. In situ study of strain-dependent ion conductivity of stretchable polyethylene oxide electrolyte. *Sci. Rep.* **2016**, *6*, 20128. DOI PubMed PMC
44. Ogawa, T.; Takahashi, K.; Kurihara, T.; et al. Network size control in coordination polymer glasses and its impact on viscosity and H^+ conductivity. *Chem. Mater.* **2022**, *34*, 5832-41. DOI
45. Frentzel-Beyme, L.; Kolodzeiski, P.; Weiß, J. B.; Schneemann, A.; Henke, S. Quantification of gas-accessible microporosity in metal-organic framework glasses. *Nat. Commun.* **2022**, *13*, 7750. DOI PubMed PMC
46. Thornton, A. W.; Jelfs, K. E.; Konstas, K.; et al. Porosity in metal-organic framework glasses. *Chem. Commun.* **2016**, *52*, 3750-3. DOI PubMed
47. Wang, Y.; Jin, H.; Ma, Q.; et al. A MOF glass membrane for gas separation. *Angew. Chem. Int. Ed. Engl.* **2020**, *59*, 4365-9. DOI PubMed

48. Bennett, T. D.; Cao, S.; Tan, J. C.; et al. Facile mechanosynthesis of amorphous zeolitic imidazolate frameworks. *J. Am. Chem. Soc.* **2011**, *133*, 14546-9. DOI PubMed
49. Zhou, C.; Longley, L.; Krajnc, A.; et al. Metal-organic framework glasses with permanent accessible porosity. *Nat. Commun.* **2018**, *9*, 5042. DOI PubMed PMC
50. Xue, W. L.; Kolodzeiski, P.; Aucharova, H.; et al. Highly porous metal-organic framework liquids and glasses via a solvent-assisted linker exchange strategy of ZIF-8. *Nat. Commun.* **2024**, *15*, 4420. DOI PubMed PMC
51. Lin, Y. Y.; Yong, A. X. B.; Gustafson, W. J.; et al. Toward design of cation transport in solid-state battery electrolytes: Structure-dynamics relationships. *Curr. Opin. Solid. State. Mater. Sci.* **2020**, *24*, 100875. DOI
52. Wang, Y.; Jiang, G.; Li, J.; et al. Glassy metal-organic framework-based solid-state electrolytes: advance, challenge, and emerging opportunities. *Small. Methods.* **2025**, *9*, e01131. DOI PubMed
53. Kong, O.; Jiang, G.; Wang, K.; et al. Elucidation of Li^+ conduction behavior in MOF glass electrolyte toward long-cycling and high C-rate lithium metal batteries. *Adv. Energy. Mater.* **2025**, *15*, 2405593. DOI
54. Kolodzeiski, P.; Gallant, B. M.; Richter, L.; et al. Alkali-ion-modified zeolitic imidazolate framework glasses. *Nature. Chem.* **2026**, *18*, 1383-92. DOI PubMed PMC
55. Ridley, P.; Nguyen, L. H. B.; Sebti, E.; et al. Amorphous and nanocrystalline halide solid electrolytes with enhanced sodium-ion conductivity. *Matter* **2024**, *7*, 485-99. DOI
56. Binci, L.; Jun, K.; Deng, B.; Ceder, G. Mechanisms of alkali ionic transport in amorphous oxyhalides solid state conductors. *arXiv* **2026**, arXiv:2601.06384. Available online: https://doi.org/10.48550/arXiv.2601.06384 (accessed 10 September 2026).
57. Nozari, V.; Calahoo, C.; Tuffnell, J. M.; et al. Sodium ion conductivity in superionic IL-impregnated metal-organic frameworks: enhancing stability through structural disorder. *Sci. Rep.* **2020**, *10*, 3532. DOI PubMed PMC
58. Zhang, H.; Zhou, Z.; Sun, X.; Zhang, Y.; Xu, H.; Gao, Y. Copper-doped metal-organic framework-74 solid-state electrolytes for high performance all-solid-state sodium metal batteries. *J. Colloid. Interface. Sci.* **2025**, *689*, 137241. DOI PubMed
59. Mirandona-Olaeta, A.; Goikolea, E.; Lanceros-Mendez, S.; Fidalgo-Marijuan, A.; Ruiz de Larramendi, I. Ionic liquid-laden Zn-MOF-74-based solid-state electrolyte for sodium batteries. *Batteries* **2023**, *9*, 588. DOI
60. Li, Z.; Gao, Y.; Wang, W.; et al. *In situ* bridging soft polymer and robust metal-organic frameworks as electrolyte for long-cycling solid-state potassium-organic batteries. *Energy. Storage. Mater.* **2024**, *72*, 103732. DOI
61. Gu, Y. J.; Lo, Y. A.; Li, A. C.; et al. A single potassium-ion conducting metal-organic framework. *ACS. Appl. Energy. Mater.* **2022**, *5*, 8573-80. DOI
62. Shannon, R. D. Revised effective ionic radii and systematic studies of interatomic distances in halides and chalcogenides. *Acta. Cryst.* **1976**, *32*, 751-67. DOI
63. Dhir, S.; Jagger, B.; Maguire, A.; Pasta, M. Fundamental investigations on the ionic transport and thermodynamic properties of non-aqueous potassium-ion electrolytes. *Nat. Commun.* **2023**, *14*, 3833. DOI PubMed PMC
64. Bennett, T. D.; Horike, S. Liquid, glass and amorphous solid states of coordination polymers and metal-organic frameworks. *Nat. Rev. Mater.* **2018**, *3*, 431-40. DOI
65. Xia, X.; Zhang, Z. Q.; Wen, Q.; et al. Metal-organic-framework-based solid-state electrolytes for high-performance lithium metal batteries: recent advances and prospects. *Chin. Chem. Lett.* **2026**, *37*, 111653. DOI
66. Kim, M.; Lee, H. S.; Seo, D. H.; Jeon, E. C.; Moon, H. R. Melt-quenched carboxylate metal-organic framework glasses. *Nat. Commun.* **2024**, *15*, 1174. DOI PubMed PMC
67. Díez, N.; Fuertes, A. B.; Sevilla, M. Molten salt strategies towards carbon materials for energy storage and conversion. *Energy. Storage. Mater.* **2021**, *38*, 50-69. DOI
68. Cao, F.; Sørensen, S. S.; Christensen, A. K. R.; et al. Continuous structure modification of metal-organic framework glasses via halide salts. *Nat. Commun.* **2025**, *16*, 7001. DOI PubMed PMC
69. Cao, F.; Sørensen, S. S.; Christensen, A. K. R.; et al. Tailoring the melting and glass transition behavior of zeolitic imidazolate frameworks via ammonium halide salts. *Small* **2026**, *22*, e73675. DOI PubMed PMC
70. Jiang, S.; Lv, T.; Peng, Y.; Pang, H. MOFs containing solid-state electrolytes for batteries. *Adv. Sci.* **2023**, *10*, e2206887. DOI PubMed PMC
71. Lim, D. W.; Kitagawa, H. Proton transport in metal-organic frameworks. *Chem. Rev.* **2020**, *120*, 8416-67. DOI PubMed
72. Chen, J.; Mei, Q.; Chen, Y.; et al. Highly efficient proton conduction in the metal-organic framework material MFM-300(Cr)·$SO_4(H_3O)_2$. *J. Am. Chem. Soc.* **2022**, *144*, 11969-74. DOI PubMed PMC
73. Ye, Y.; Guo, W.; Wang, L.; et al. Straightforward loading of imidazole molecules into metal-organic framework for high proton conduction. *J. Am. Chem. Soc.* **2017**, *139*, 15604-7. DOI PubMed
74. Ramaswamy, P.; Wong, N. E.; Shimizu, G. K. H. MOFs as proton conductors - challenges and opportunities. *Chem. Soc. Rev.* **2014**, *43*, 5913-32. DOI PubMed
75. Lim, D. W.; Kitagawa, H. Rational strategies for proton-conductive metal-organic frameworks. *Chem. Soc. Rev.* **2021**, *50*, 6349-68. DOI PubMed
76. Meng, X.; Wang, H. N.; Song, S. Y.; Zhang, H. J. Proton-conducting crystalline porous materials. *Chem. Soc. Rev.* **2017**, *46*, 464-80. DOI PubMed

77. Urgoiti-Rodriguez, M.; Vaquero-Vílchez, S.; Mirandona-Olaeta, A.; et al. Exploring ionic liquid-laden metal-organic framework composite materials as hybrid electrolytes in metal (ion) batteries. *Front. Chem.* **2022**, *10*, 995063. DOI PubMed PMC
78. Yoshida, Y.; Kitagawa, H. Ionic conduction in metal-organic frameworks with incorporated ionic liquids. *ACS. Sustainable. Chem. Eng.* **2019**, *7*, 70-81. DOI
79. Xiang, Y.; Yu, N.; Li, J.; et al. Carving metal-organic-framework glass based solid-state electrolyte via a top-down strategy for lithium-metal battery. *Angew. Chem. Int. Ed. Engl.* **2025**, *64*, e202424288. DOI PubMed
80. Yoshida, Y.; Fujie, K.; Lim, D. W.; Ikeda, R.; Kitagawa, H. Superionic conduction over a wide temperature range in a metal-organic framework impregnated with ionic liquids. *Angew. Chem. Int. Ed. Engl.* **2019**, *58*, 10909-13. DOI PubMed
81. Ding, J.; Du, T.; Thomsen, E. H.; et al. Metal-organic framework glass as a functional filler enables enhanced performance of solid-state polymer electrolytes for lithium metal batteries. *Adv. Sci.* **2024**, *11*, e2306698. DOI PubMed PMC
82. Liu, S.; Jiang, G.; Wang, Y.; et al. Vitrified metal-organic framework composite electrolyte enabling dendrite-free and long-lifespan solid-state lithium metal batteries. *ACS. Nano.* **2024**, *18*, 14907-16. DOI PubMed
83. Wang, C.; Zhang, J.; Shi, P.; Zhou, Z.; Zhang, Y.; Gao, Y. Metal organic framework MOF-808-based solid-state electrolytes for lithium-ion batteries. *New. J. Chem.* **2023**, *47*, 14114-7. DOI
84. Wang, K.; Yang, L.; Wang, Z.; et al. Enhanced lithium dendrite suppressing capability enabled by a solid-like electrolyte with different-sized nanoparticles. *Chem. Commun.* **2018**, *54*, 13060-3. DOI PubMed
85. Wang, Z.; Wang, Z.; Yang, L.; et al. Boosting interfacial Li^+ transport with a MOF-based ionic conductor for solid-state batteries. *Nano. Energy.* **2018**, *49*, 580-7. DOI
86. Wang, Z.; Tan, R.; Wang, H.; et al. A metal-organic-framework-based electrolyte with nanowetted interfaces for high-energy-density solid-state lithium battery. *Adv. Mater.* **2018**, *30*, 1704436. DOI PubMed
87. Wu, J. F.; Guo, X. Nanostructured metal-organic framework (MOF)-derived solid electrolytes realizing fast lithium ion transportation kinetics in solid-state batteries. *Small* **2019**, *15*, e1804413. DOI PubMed
88. Abdelmaoula, A. E.; Shu, J.; Cheng, Y.; et al. Core-shell MOF-in-MOF nanopore bifunctional host of electrolyte for high-performance solid-state lithium batteries. *Small. Methods.* **2021**, *5*, e2100508. DOI PubMed
89. Zettl, R.; Hanzu, I. The origins of ion conductivity in MOF-ionic liquids hybrid solid electrolytes. *Front. Energy. Res.* **2021**, *9*, 714698. DOI
90. Yu, X.; Grundish, N. S.; Goodenough, J. B.; Manthiram, A. Ionic liquid (IL) laden metal-organic framework (IL-MOF) electrolyte for quasi-solid-state sodium batteries. *ACS. Appl. Mater. Interfaces.* **2021**, *13*, 24662-9. DOI PubMed
91. Ferbezar, A.; Zettl, R.; Fitzek, H.; Gadermaier, B.; Hanzu, I. Ion conduction in Na^+ containing ionogels based on the UiO-66 metal organic framework. *Electrochim. Acta.* **2022**, *434*, 141212. DOI
92. Xue, W. L.; Li, G. Q.; Chen, H.; et al. Melt-quenched glass formation of a family of metal-carboxylate frameworks. *Nat. Commun.* **2024**, *15*, 2040. DOI PubMed PMC
93. Tian, X.; Yi, Y.; Wu, Z.; et al. Ionic liquid confined in MOF/polymerized ionic network core-shell host as a solid electrolyte for lithium batteries. *Chem. Eng. Sci.* **2023**, *266*, 118271. DOI
94. He, C.; Sun, J.; Hou, C.; et al. Sandwich-structural ionogel electrolyte with core-shell ionic-conducting nanocomposites for stable Li metal battery. *Chem. Eng. J.* **2023**, *451*, 138993. DOI
95. Ma, N.; Kosasang, S.; Yoshida, A.; Horike, S. Proton-conductive coordination polymer glass for solid-state anhydrous proton batteries. *Chem. Sci.* **2021**, *12*, 5818-24. DOI PubMed PMC
96. Majid, M. F.; Mohd Zaid, H. F.; Kait, C. F.; Ahmad, A.; Jumbri, K. Ionic liquid@metal-organic framework as a solid electrolyte in a lithium-ion battery: current performance and perspective at molecular level. *Nanomaterials* **2022**, *12*, 1076. DOI PubMed PMC
97. Nozari, V.; Calahoo, C.; Tuffnell, J. M.; Keen, D. A.; Bennett, T. D.; Wondraczek, L. Ionic liquid facilitated melting of the metal-organic framework ZIF-8. *Nat. Commun.* **2021**, *12*, 5703. DOI PubMed PMC
98. Longley, L.; Collins, S. M.; Li, S.; et al. Flux melting of metal-organic frameworks. *Chem. Sci.* **2019**, *10*, 3592-601. DOI PubMed PMC
99. Thorne, M. F.; Gómez, M. L. R.; Bumstead, A. M.; Li, S.; Bennett, T. D. Mechanochemical synthesis of mixed metal, mixed linker, glass-forming metal-organic frameworks. *Green. Chem.* **2020**, *22*, 2505-12. DOI
100. Madsen, R. S. K.; Stepniewska, M.; Yang, Y.; et al. Mixed metal node effect in zeolitic imidazolate frameworks. *RSC. Adv.* **2022**, *12*, 10815-24. DOI PubMed PMC
101. León-Alcaide, L.; Christensen, R. S.; Keen, D. A.; et al. Meltable, glass-forming, iron zeolitic imidazolate frameworks. *J. Am. Chem. Soc.* **2023**, *145*, 11258-64. DOI PubMed PMC
102. Azbell, T. J.; Pitt, T. A.; Bollmeyer, M. M.; Cong, C.; Lancaster, K. M.; Milner, P. J. Ionothermal synthesis of metal-organic frameworks using low-melting metal salt precursors. *Angew. Chem. Int. Ed. Engl.* **2023**, *62*, e202218252. DOI PubMed PMC

103. Bode, T.; Xue, W. L.; Garcia Alvarez, K. M.; et al. Defect identification in zeolitic imidazolate framework glasses by solid-state NMR spectroscopy using $^{13}CO_2$ as probe. *Chem. Mater.* **2025**, *37*, 1578-87. DOI
104. Shalini, S.; Vaid, T. P.; Matzger, A. J. Salt nanoconfinement in zirconium-based metal-organic frameworks leads to pore-size and loading-dependent ionic conductivity enhancement. *Chem. Commun.* **2020**, *56*, 7245-8. DOI PubMed
105. Farina, M.; Duff, B. B.; Tealdi, C.; Pugliese, A.; Blanc, F.; Quartarone, E. Li^+ dynamics of liquid electrolytes nanoconfined in metal-organic frameworks. *ACS. Appl. Mater. Interfaces.* **2021**, *13*, 53986-95. DOI PubMed PMC
106. Butreddy, P.; Wijesingha, M.; Laws, S.; Pathiraja, G.; Mo, Y.; Rathnayake, H. Insight into the isoreticularity of Li-MOFs for the design of low-density solid and quasi-solid electrolytes. *Chem. Mater.* **2023**, *35*, 9857-78. DOI PubMed PMC
107. Longley, L.; Calahoo, C.; Limbach, R.; et al. Metal-organic framework and inorganic glass composites. *Nat. Commun.* **2020**, *11*, 5800. DOI PubMed PMC
108. Chen, W.; Horike, S.; Umeyama, D.; et al. Glass formation of a coordination polymer crystal for enhanced proton conductivity and material flexibility. *Angew. Chem. Int. Ed.* **2016**, *55*, 5195-200. DOI PubMed
109. Bischoff, C.; Schuller, K.; Beckman, S. P.; Martin, S. W. Non-arrhenius ionic conductivities in glasses due to a distribution of activation energies. *Phys. Rev. Lett.* **2012**, *109*, 075901. DOI PubMed
110. Murugavel, S.; Vaid, C.; Bhadram, V. S.; Narayana, C. Ion transport mechanism in glasses: non-arrhenius conductivity and nonuniversal features. *J. Phys. Chem. B.* **2010**, *114*, 13381-5. DOI PubMed
111. Riess, I. Four point Hebb-Wagner polarization method for determining the electronic conductivity in mixed ionic-electronic conductors. *Solid. State. Ionics.* **1992**, *51*, 219-29. DOI
112. Lee, K. R.; Lee, J. H.; Yoo, H. I. Reassessment of conventional polarization technique to measure partial electronic conductivity of electrolytes. *Solid. State. Ionics.* **2010**, *181*, 724-9. DOI
113. Shao, B.; Huang, Y.; Han, F. Electronic conductivity of lithium solid electrolytes. *Adv. Energy. Mater.* **2023**, *13*, 2204098. DOI
114. Hou, T.; Xu, W.; Pei, X.; Jiang, L.; Yaghi, O. M.; Persson, K. A. Ionic conduction mechanism and design of metal-organic framework based quasi-solid-state electrolytes. *J. Am. Chem. Soc.* **2022**, *144*, 13446-50. DOI PubMed PMC
115. Rehr, J. J.; Albers, R. C. Theoretical approaches to x-ray absorption fine structure. *Rev. Mod. Phys.* **2000**, *72*, 621-54. DOI
116. Chantler, C. T.; Bunker, G.; D'Angelo, P.; Diaz-Moreno, S. X-ray absorption spectroscopy. *Nat. Rev. Methods. Primers.* **2024**, *4*, 89. DOI
117. Laulainen, J. E. M.; Johnstone, D. N.; Bogachev, I.; et al. Mapping short-range order at the nanoscale in metal-organic framework and inorganic glass composites. *Nanoscale* **2022**, *14*, 16524-35. DOI PubMed
118. Keen, D. A. Total scattering and the pair distribution function in crystallography. *Crystallogr. Rev.* **2020**, *26*, 143-201. DOI
119. Billinge, S. J. L. The rise of the X-ray atomic pair distribution function method: a series of fortunate events. *Philos. Trans. A. Math. Phys. Eng. Sci.* **2019**, *377*, 20180413. DOI PubMed PMC
120. Peterson, P. F.; Olds, D.; Mcdonnell, M. T.; Page, K. Illustrated formalisms for total scattering data: a guide for new practitioners. *J. Appl. Crystallogr.* **2021**, *54*, 317-32. DOI PubMed PMC
121. Molina, M. A.; Manjón-Sanz, A.; Sánchez-Sánchez, M. On the contribution of Pair Distribution Function (PDF) to the characterization of nanocrystalline MOFs: the case of M-MOF-74. *Microporous. Mesoporous. Mater.* **2021**, *319*, 110973. DOI
122. Hou, J.; Chen, P.; Shukla, A.; et al. Liquid-phase sintering of lead halide perovskites and metal-organic framework glasses. *Science* **2021**, *374*, 621-5. DOI PubMed
123. Lin, R.; Li, X.; Krajnc, A.; et al. Mechanochemically synthesised flexible electrodes based on bimetallic metal-organic framework glasses for the oxygen evolution reaction. *Angew. Chem.* **2022**, *134*, e202112880. DOI
124. Zhao, Z.; Ding, L.; Mundstock, A.; et al. Preparation of ZIF-62 polycrystalline and glass membranes for helium separation. *J. Membr. Sci.* **2024**, *700*, 122677. DOI
125. Wang, Y.; Wu, J.; Li, Z.; et al. Scalable glass composite membranes for highly selective lithium enrichment. *Nat. Water.* **2026**, *4*, 643-55. DOI
126. Wang, J.; Panchal, A. A.; Sai Gautam, G.; Canepa, P. The resistive nature of decomposing interfaces of solid electrolytes with alkali metal electrodes. *J. Mater. Chem. A.* **2022**, *10*, 19732-42. DOI
127. Zhu, Y.; He, X.; Mo, Y. Origin of outstanding stability in the lithium solid electrolyte materials: insights from thermodynamic analyses based on first-principles calculations. *ACS. Appl. Mater. Interfaces.* **2015**, *7*, 23685-93. DOI PubMed
128. Cao, D.; Sun, X.; Li, Q.; Natan, A.; Xiang, P.; Zhu, H. Lithium dendrite in all-solid-state batteries: growth mechanisms, suppression strategies, and characterizations. *Matter* **2020**, *3*, 57-94. DOI